Distribution Statement

Distribution A: Public Release.

The views presented here are those of the author and are not to be construed as official or reflecting the views of the Uniformed Services University of the Health Sciences, the Department of Defense or the U.S. Government.

Effects of Intranasal Insulin on Controlled Cortical Impact Brain Injury in a Rat Model

by

John Richard Reed

Dissertation submitted to the Faculty of the
Neuroscience Graduate Program
Uniformed Services University of the Health Sciences
In partial fulfillment of the requirements for the degree of
Doctor of Philosophy 2019

UNIFORMED SERVICES UNIVERSITY OF THE HEALTH SCIENCES
SCHOOL OF MEDICINE GRADUATE PROGRAMS
Graduate Education Office (A 1045), 4301 Jones Bridge Road, Bethesda, MD 20814

APPROVAL OF THE DOCTORAL DISSERTATION IN THE NEUROSCIENCE GRADUATE PROGRAM

Title of Dissertation: "Effects of Intranasal Insulin on CCI in a Rat Model"

Name of Candidate: John R. Reed
Doctor of Philosophy Degree
June 27, 2019

DISSERTATION AND ABSTRACT APPROVED:

DATE:

_____ _____
Dr. Joseph McCabe
DEPARTMENT OF ANATOMY, PHYSIOLOGY & GENETICS
Committee Chair

_____ _____
Dr. Kimberly Byrnes
DEPARTMENT OF ANATOMY, PHYSIOLOGY & GENETICS
Dissertation Advisor

_____ _____
Dr. Martin Doughty
DEPARTMENT OF ANATOMY, PHYSIOLOGY & GENETICS
Committee Member

_____ _____
Dr. Kwang H. Choi
DEPARTMENT OF PSYCHIATRY
Committee Member

_____ _____
Dr. Andrew L. Snow
DEPARTMENT OF PHARMACOLOGY & MOLECULAR THERAPEUTICS
Committee Member

ACKNOWLEDGMENTS

This dissertation is the result of tremendous amount of work, support, and patience by many people at USUHS. First I want to thank my mentor, Dr. Kimberly Byrnes for agreeing to take me on in your lab. Thank you for all of your time and patience in helping me to get through this project and this program. I can't imagine the frustration you felt teaching this old dog new tricks but your support and encouragement were instrumental in my success. I would also like to thank the members of my dissertation committee, Dr. Joseph McCabe, committee chair, Dr. Martin Doughty, Dr. Kwang Choi, and Dr. Andrew Snow. You shared in guiding me down a path I often found difficult to navigate. I would like to also acknowledge Dr. Cara Olsen, who provided invaluable guidance for the statistical analysis of my data.

Thank you to the entire Byrnes' lab past and present, you have been a wonderful and supportive group that I will truly miss – Fiona Brabazon, PhD, Ramona Von-Leden PhD, LTC John Yauger, PhD, Nicole Hockenbury, Michael Shaughness, Deanna Acs, and Sarah Bermudez, as well as others around the lab, LTC Michael Neill, PhD, Guzal Khayrullina, Samantha Scott and the entire graduate department. You have all been open with valuable insight when asked.

Dr. Tao-Yiao Wu, thank you for serving as my qualification committee chair and continuing to offer assistance with my behavioral studies. Dr. Mumeko Tsuda, thank you for all of your assistance prepping, running, evaluating, and discussion my behavior tests. Your assistance and insight was very helpful.

Thank you to the Kortum lab Robert Kortum, PhD, Erin Sheffels, Patricia Theard, and Nancy Sealover, for patiently answering all of my many signaling questions.

I would like to thank Dr. Amanda Fu, Laura Tucker, Dr. Jiong Liu, Dr. Dennis McDaniel, Kateryna Lund, Lisa Meyers, Shalini Jaiswal, Alexandru Korotcov, PhD, and Bernard Dardzinski, PhD for your assistance and guidance in all of my endeavors with surgery, radiology, cytometry, and histology.

And my classmates, LTC Peter Attilio, Nikki McCormack, and Eileen McNamara, thank you for your comradery through this ordeal. I hope we can stay in touch.

Thank you to the tri-services nursing research program (TSNRP) for the generous grant used to fund this project as well as the travel to disseminate the information.

Finally, I would like to thank my family and friends for your support.

DEDICATION

This dissertation is dedicated to my family. My wife, and best friend, Kelly, and our 4 children, Kaitlyn, Ryan, Collin, and Liam, you all mean everything to me. My Mom, Dad, and little sister who always supported me, pushed me, loved me, and inspired me.

Thank you all!

COPYRIGHT STATEMENT

The author hereby certifies that the use of any copyrighted material in the dissertation manuscript entitled: Effects of Intranasal Insulin on Controlled Cortical Impact Brain Injury in a Rat Model is appropriately acknowledged and, beyond brief excerpts, is with the permission of the copyright owner.

[Signature]

John R. Reed

July 22, 2019

DISCLAIMER

The views presented here are those of the author and are not to be construed as official or reflecting the views of the Uniformed Services University of the Health Sciences, the Department of Defense or the U.S. Government.

ABSTRACT

Effects of Intranasal Insulin on CCI in a Rat Model:

John R. Reed, Doctor of Philosophy, 2019

Thesis directed by: Kimberly R. Byrnes, PhD

Department of Anatomy, Physiology and Genetics

Professor, Program Director, Neuroscience Program

Traumatic brain injury (TBI) is a serious health problem that affects approximately 2.5 million people in the United States each year and causes serious cognitive and physical deficits lasting long after the acute injury. Physical and cognitive limitations, as well as anxiety, have been identified as common and critical issues after TBI. One of the subcortical structures that is often damaged and is classically linked to memory and anxiety is the hippocampus. TBI results in a marked reduction in glucose uptake in the brain, including in the hippocampus, which can last for years after injury. Currently, there is no effective treatment devised for the deficits that develop after TBI. An additional complication is gaining access of the treatment to the central nervous system (CNS) because of the protection from the blood-brain barrier (BBB). Research has demonstrated that some drugs, such as insulin, can reach the CNS by intranasal administration through the olfactory and trigeminal pathways. Intranasal insulin administration has been shown to increase cerebral glucose uptake and improve memory

function in normal subjects and patients with Alzheimer's disease, without affecting systemic blood glucose or insulin levels. Our previous work demonstrated that after a moderate TBI in rats, intranasal insulin administered within 4 hours after injury significantly increased glucose uptake in the hippocampus, improved cognitive function, and reduced inflammation. However, the mechanism by which insulin has these effects and the temporal course of these effects is currently unclear. The goal of this study was to determine if intranasal insulin administration would reduce inflammation and neuronal loss in the hippocampus and reduce measures of anxiety in rats exposed to moderate TBI. We also wanted to evaluate the mechanism by which intranasal insulin administration affects the hippocampus. To accomplish these goals, adult male Sprague Dawley rats were exposed to a moderate controlled cortical impact (CCI) injury. Intranasal insulin treatments were administered 4 hours after injury and then daily for 14 days. Multiple behavior tests, including open field, elevated zero maze and light-dark box, were used to assess anxiety. Histological analysis with NeuN was used to assess total number of neurons in the hippocampus. In order to assess inflammation, microglial/macrophage number and activation in the hippocampus was measured as well as the production of cytokines. We found that intranasal insulin did not have a significant effect on neuronal (NeuN) or microglial/macrophage (Iba1) density, but did decrease expression of CD86, iNOS, and TNFα within the hippocampus at specific time points post injury. Cellular signaling demonstrated that intranasal insulin increased the phosphorylated MEK to total MEK ratio in the cortex 4 days post injury. With this model, TBI did not increase anxiety-like behavior when compared to sham, negating the ability to evaluate treatment. This is possibly due to the neuroprotective properties of isoflurane provided to both

groups during surgery and treatment. These data indicate that there is an effect on pro-inflammatory factors and the MAPK pathway that may play a role in intranasal insulin's effect after TBI.

These data add to the body of knowledge as to the mechanism of the effect of intranasal insulin after TBI. And though it falls short on giving any therapeutic insight for the treatment of anxiety, it does bring up some ideas for how to change the research paradigm in order to better evaluate this potential therapy in future experiments. Intranasal insulin clearly decreases pro-inflammatory molecules that have been shown to be causes of pathogenesis.

TABLE OF CONTENTS

LIST OF TABLES

LIST OF FIGURES

CHAPTER 1: Introduction

TRAUMATIC BRAIN INJURY

Traumatic brain injury (TBI) is a serious health problem that accounts for over 2.5 million emergency room visits, hospitalizations, and deaths in the United States each year and causing serious cognitive and physical deficits lasting long after the initial injury (13; 78). The Centers for Disease Control and Prevention (CDC) defines traumatic brain injury (TBI) as an injury that disrupts the normal function of the brain that negatively affects the quality of life cognitively, emotionally, behaviorally, physically, socially, and occupationally (78). In the general population, falls (35%), motor vehicle-related accidents (17%) and blows to the head (17%) are the most common causes (77). Though the young (0-4 years), adolescent (15-19 years) and elderly (75+ years) are the most likely, to sustain a TBI in civilians, a critical need is also seen where, from 2000 to 2011, over 4% of the total armed forces have been diagnosed with a TBI. These numbers do not account for the many other injuries that go unreported.

TBI results in damage through direct contact with the skull, shearing forces, or an object penetrating the skull (4; 13; 98). The primary injury can be categorized as focal (localized) or diffuse (widespread), although clinicians recognize this distinction is arbitrary, and refers to morphological observations (3). A focal injury, like the one used in this dissertation, is an injury that is specific in its area of impact (87). This can be seen in bleeding or bruising as in a coup, contra coup injury where the brain strikes the interior of the skull(3). Another example of a focal injury is a penetrating injury where an object has actually penetrated the skull and entered into or through the brain (61). A diffuse injury is one that disperses the area of injury (AOI) throughout the brain and is more likely in a blast injury if the subject does not strike the head after a fall (87). This is also

described as non-penetrating or closed head injury where there is no direct impact with the brain tissue (74).

TBI is also characterized by the pathological changes in diverse cortical areas, subcortical nuclei, and white matter tracts that follow traumatic injury (44). The pathological changes include the primary effects, focal and diffuse, described above as well as secondary damage such as vasogenic edema, cytotoxic edema and fluctuations in metabolic and immune processes (13; 61; 100). The fluctuation in metabolic processes includes an initial hypermetabolic state and then a significant reduction in cerebral glucose uptake that slowly increases over time back to normal glucose uptake values (11). Research shows that both the initial hypermetabolic state (47) and the chronic state of reduced glucose uptake correlate with negative long term outcomes (11; 34; 36; 54). Beyond the basic cellular demands (i.e. ATP production), glucose is essential for maintenance of the membrane potential, information processing, neural computation, and neurotransmitter production (11; 38; 65). Because it plays a critical role in brain function, and disruption of normal glucose metabolism is a basis for many neurologic disorders, there is need for tight regulation of glucose in the brain (65). Though the human brain accounts for only 2% of the total body weight, it is estimated that it requires at least 20% of the body's glucose (65).

CONTROLLED CORTICAL IMPACT

In order to investigate TBI, a number of animal models have been developed, such as the controlled cortical impact (CCI) model. CCI is an effective tool that has become one of the most commonly used mechanical models for TBI since it was developed in the late 1980's (27; 74). It gives the opportunity to investigate many

aspects of TBI that include derangements of microanatomy, disruption of the blood-brain barrier, hematomas, edema, inflammation and alterations in blood flow (27; 74). The injury can be inflicted with a high level of control and reproducibility with measurable specified impact parameters (velocity, depth, duration, and impact site) (27). In addition to the noted injury to the brain tissue, functional deficits have been noted and used for behavioral testing like MWM, EZM and beam walk (11; 27; 74). However, CCI is not without limitations that need to be accounted for when using this model. There are arguments that the injury is not clinically relevant as most TBIs do not come with a craniotomy or craniectomy, a direct impact focal injury, and use of anesthesia (27).

GLUCOSE USE BY THE BRAIN

In order for glucose to reach the brain, it must first cross the blood brain barrier (BBB) (29; 65). In a healthy state, the unique structure of the BBB results in minimal permeability to large non-lipophilic molecules from blood to the central nervous system (CNS) parenchyma (75). The BBB is a specialized vascular structure tightly regulating CNS homeostasis (2). It consists of endothelial cells, astrocytes, pericytes, a variety of basement membranes, and smooth muscle (2; 29).

Glucose transporters (GLUTs) are transmembrane proteins that are used for facilitated transport of glucose across the BBB as well as into cells (65; 85). Increasing cerebral glucose uptake has been shown to significantly improve outcome after TBI (11; 103). There are 5 members of the GLUT family. GLUT1 transporters are described as ubiquitous as they are located in tissues throughout the body (85). They are located in the BBB and the plasma membrane of the oligodendrocytes, astroglia, and microglia that support the neurons within the CNS (65; 85). GLUT3 transporters are located within the

plasma membranes of CNS neurons and have a higher rate of glucose transport to try to keep up with the increased energy needs (65). GLUT4 are insulin sensitive transporters located within the CNS on neurons, microglia and astrocytes (42; 45; 66). GLUT4 transporters are unique in that they start intracellularly in the absence of insulin, and then through endo and exocytosis, decrease or increase expression within the cell membrane with insulin stimulation (85).

INSULIN EFFECTS ON GLUCOSE IN THE BRAIN

Insulin is an anabolic hormone that is secreted by the pancreas and causes cells to take up energy substrates in times of excess. Insulin's action on the cell is mediated by the insulin receptor (IR) (77; 81; 84). The IR is a large, heterodimeric transmembrane glycoprotein, consisting of 719 or 731 amino acids, and belonging to the receptor tyrosine kinase (RTK) family (77; 81; 84). IR has been shown to be reduced in patients suffering from Alzheimer's disease (37), and its expression following TBI is currently unclear, though insulin resistance has been noted as an exacerbating factor in TBI (46), and it has been reported that IRs can be phosphorylated and inactivated as a result of TBI (46).

It has also been reported that IRs are not evenly distributed throughout the brain (105). Instead, they are concentrated in discrete regions, including the hippocampus (105). Insulin has been noted to increase glucose uptake in the rat hippocampus (12) and improve neuronal survival *in vitro*, through the IR signaling pathway, when cells are stressed by glucose deprivation (101).

Insulin binds to a portion of the IR known as the insulin-binding domain (84) (Fig. 1).

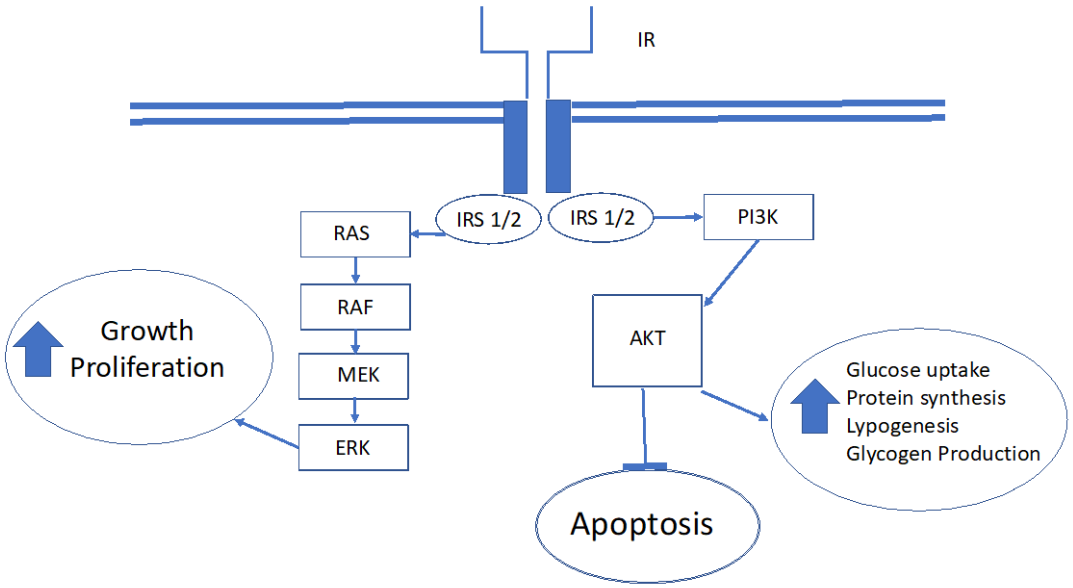

Fig. 1 – Insulin receptor signaling pathway. When stimulated, the insulin receptor (IR), a receptor tyrosine kinase (RTK) dimerizes and leads to rapid auto phosphorylation of the receptor, followed by tyrosine phosphorylation of insulin receptor substrate (IRS) proteins and then activating downstream pathways such as the PI3K and the mitogen-activated protein kinase (MAPK) cascades. The PI3K pathway is associated with metabolic and survival (anti-apoptotic) processes, while the MAPK pathway is associated with growth and proliferation.

The binding of insulin to the IR leads to rapid auto phosphorylation of the receptor (77; 81; 84). This, in turn, is followed by tyrosine phosphorylation of insulin receptor substrate (IRS) proteins and activation of signaling pathways such as the PI3K and the mitogen-activated protein kinase (MAPK) cascades (77; 81; 84).

Insulin can directly affect a number of neuronal functions, including neurite outgrowth, survival, differentiation, migration, energy metabolism, gene expression, protein synthesis, cytoskeletal assembly, synapse formation, neurotransmitter function, and plasticity (30; 56; 80). This can be achieved through either activation of the PI3K/AKT pathway and glucose transporter (GLUT) activation (92), or through

alternative mechanisms such as the MAPK signal transduction pathway (102) (Fig. 1).

Our previously published data demonstrates that intranasal insulin increases glucose uptake in the brain after moderate TBI in a rat model, and improves cognitive function (11). However, it is not clear if these actions are through the IR, if these effects are region specific, or if these effects are mediated by neurons or microglial cells.

INTRANASAL INSULIN

The intranasal route of medication administration has gained a lot of interest over the past decade (19). It gives the ability to non-invasively and directly access the CNS (19). Due to the large size and polarity, the insulin molecule cannot cross directly into the bloodstream from the nasal cavity (67). Because it is not absorbed into the mucus membranes, it is able to pass into the upper portion of the nasal cavity and access the CNS (19).

When given intranasally, insulin accesses the CNS by following the olfactory and trigeminal cranial nerves to the rostral and caudal brain, respectively, through intracellular and extracellular means (19). Because intracellular transport would take hours to days and the onset of extracellular transport is very rapid it is thought that the extracellular pathway through paracellular diffusion is responsible for the therapeutic effect (19; 60). Once reaching the CNS, research has shown that insulin permeates the entire brain and has no effect on blood glucose or weight (11; 37).

IMPACT OF TBI - HIPPOCAMPUS

One of the subcortical structures that is often damaged and is classically linked to memory and anxiety is the hippocampus (12; 25; 43; 50). This damage to the hippocampus is reflected by hippocampal lesion formation (50), atrophy (5), and

neuronal loss (12). The effects of TBI on the hippocampus have been shown via increased edema and reduced glucose uptake starting just hours to days after injury and continuing for several months (11; 15; 20; 57). Our previous studies demonstrated an increase in edema volume within the hippocampus after TBI at both 3 and 9 days post injury (11).

The hippocampus is an important part of the limbic system and one of the most studied areas of the brain (33). It is a seahorse-shaped structure involved in learning, memory, and emotion (33). The association of the hippocampus and memory was established in the 1950s with a patient known as "HM" (33; 88). HM suffered from seizures that were eventually treated with surgery that removed his medial temporal lobes that included his hippocampi, and subsequently he experienced profound memory impairments (33; 88). This association is key to our research as we are looking into the mechanism of increased memory, as well as the potential for impact on TBI-induced anxiety (11). The injury site is located directly over the CA1 (CA derived from cornu ammonis) region of the hippocampus for our CCI model (Chapter 2). The CA1 region was chosen for this research as it is most closely associated with memory (70).

IMPACT OF TBI - ANXIETY

In addition to physical and cognitive limitations, anxiety has also been identified as a common and critical issue (73; 83). As described in the previous section, the hippocampus is subcortical structure often damaged in TBI. Damage to the hippocampus is associated with increased anxiety in humans (50). Injury to the hippocampus is also associated with increased anxiety-like behavior in rats (7). The hippocampus is also involved in the regulation of the hypothalamic-pituitary-adrenal (HPA) axis (9; 39; 64).

The HPA axis is vital for the proper regulation of energy during times of stress (9). Disturbances in the HPA axis constitute a leading cause of long-term sequela after TBI (58) and are also associated with anxiety and stress (28; 97; 98). This can be seen through the elevation of stress-related hormones including cortisol in humans or corticosterone (CORT) in rodents (82). The impact the hippocampus has on anxiety is derived from a direct link between the hippocampus and the hypothalamus (43).

Intranasal insulin has also been used in rats to reverse anxiety-like responses and hippocampal neuroinflammation that were induced through methamphetamine administration (7). Further, research from our laboratory has shown that intranasal insulin increases glucose uptake, and has a significant impact on edema in the hippocampus (11), which might impact anxiety in the same way we observed impacts on memory.

IMPACT OF TBI - INFLAMMATION

Microglia are distributed throughout the CNS and are the resident macrophage-like cells of the CNS (21). Microglia comprise approximately 15% of the cell population of the CNS and share many similarities to peripheral macrophages (16). Microglia maintain homeostasis in the CNS through actively sensing the surrounding environment (51; 69; 90). Though described as “resting”, microglia are very mobile and active in the surveillance of the surrounding environment, making use of their very long, thin processes that cover the entire brain parenchyma (21). The processes contain pattern recognition receptors that respond to pathogen-associated molecular patterns (PAMPs) or damage-associated molecular patterns (DAMPs) that indicate a potential infection or injury (21; 53; 59). The alterations in immune response induced by TBI include a

significant elevation in microglial activation that begins at about 24 hours post-injury and peaks at 4–7 days post-injury (59). This response is supplemented by the entry of peripheral neutrophils, macrophages, and lymphocytes with the rupture of the blood brain barrier (53). The neutrophils have an early onset and peak during the initial 24 hours (6). But as the neutrophil numbers decrease during the first couple of days, the macrophages follow a similar timeline to that of microglia, peaking at 4-7 days (6). Microglial activation is when the microglia go from a ramified, resting state with a dendritic morphology to an ameboid morphology resembling blood borne macrophages in response to injury (59). This morphological change is combined with behavior in that the microglia goes from monitoring to an active state where it proliferates and migrates to the site of injury (59).

It has been shown that microglia are activated in response to TBI with both pro-inflammatory (M1, classical activation) and anti-inflammatory (M2, alternative activation) effects (11; 13; 21; 22; 36; 59; 68). Pro-inflammatory microglia display M1 phenotypic markers (i.e. CD86, iNOS) and are associated with phagocytosis, release of reactive oxygen species (ROS), nitric oxide (NO), and production of pro-inflammatory cytokines (i.e. TNFα, IL1B, IL6). Pro-inflammatory activation of microglia has been shown to have neurotoxic effects (22; 59; 68) as well as promote insulin resistance, further promoting secondary injury and blocking cellular protective pathways (46). The anti-inflammatory microglia display M2 phenotypic markers (i.e. CD206) and release anti-inflammatory cytokines that are neuroprotective (i.e. IL10) (21).

TBI – INSULIN AS A THERAPEUTIC

To date, there are no clinically available therapeutics that address either the initial

or secondary injury associated with TBI. A multi-pronged therapeutic that can directly access the brain may be optimal for treatment of TBI. In 2008, Dr. William Frey II's group at the University of Minnesota reported that intranasal insulin was effective in improving memory for patients suffering from Alzheimer's disease, and the patients suffered no adverse effects of decreased blood sugar (37).

When given intranasally, insulin accesses the CNS by following the olfactory and trigeminal cranial nerves to the rostral and caudal brain, respectively, through intracellular and extracellular means (19). Because intracellular transport would take hours to days and the onset of extracellular transport is very rapid it is thought that the extracellular pathway is responsible for the therapeutic effect (19). Once reaching the CNS, our lab has shown that it permeates the entire brain and has no effect on blood glucose or weight (11). Intranasal insulin has been shown to be a promising method for decreasing microglial-induced inflammation in the CNS (7; 11). With the decrease in inflammation, this therapy has also shown potential to decrease anxiety (7) and improve memory in both rats (11) and humans (19).

With this background in mind, the purpose of this study was to evaluate the mechanism by which intranasal insulin administration affects the hippocampus and broaden its therapeutic potential for treatment of TBI in a rat model. We hypothesized that **intranasal insulin administration will reduce inflammation and neuronal loss in the hippocampus and reduce measures of anxiety in rats exposed to moderate TBI.** To test this hypothesis, we proposed the following three specific aims:

Aim 1: **To demonstrate that intranasal insulin administration will reduce anxiety-like symptoms associated with TBI.** *We hypothesized that intranasal insulin*

administration would reduce anxiety-like behavior. TBI results in an increase in anxiety-like behavior in rats (55; 57); this function is correlated with hippocampal damage (12; 25; 43; 50). We proposed to test this hypothesis utilizing behavioral testing via the light-dark box, elevated zero maze, and open field test following moderate TBI and insulin administration.

Aim 2: **To determine the effects of intranasal insulin on hippocampal neuronal viability.** *We hypothesized that intranasal insulin would reduce neuronal damage in the hippocampus after moderate TBI.* Our preliminary data indicated that intranasal insulin had significant effects in the injured hippocampus and hippocampal related function to include improvements of memory and decreased edema volume in this area(11). However, it was unclear if these benefits were mediated by insulin-mediated metabolic or non-metabolic signal transduction pathway activation leading to elevated neuronal survival. Therefore, we investigated IR signaling pathways by assessing phosphorylation of AKT and MAPK. We performed histological analysis with the marker, NeuN to evaluate the total number of neurons in the hippocampus.

Aim 3: **To assess microglial changes in the hippocampus after intranasal insulin administration.** *We hypothesized that the addition of intranasal insulin would decrease microglial-related inflammation after TBI.* Microglia are the resident macrophage-like cells of the brain and serve an important purpose in the acute stages following TBI that include clearing cellular debris. However, it has been shown that prolonged activation can be detrimental due to the release of pro-inflammatory cytokines, nitric oxide, and reactive oxygen species that can result in neuronal cell death[22]. In order

to assess inflammation, we used commercially available antibodies to assess microglial number and activation in the hippocampus

Previous research has demonstrated that intranasal insulin improves outcomes after TBI. This proposal will help to clarify the mechanism of these effects and provide more information on therapeutic targets. These data will be essential for the development of a future clinical trial.

CHAPTER 2: Methods

CONTROLLED CORTICAL IMPACT INJURY (CCI)

Adult male Sprague–Dawley rats (250–350 g; Taconic, Germantown, NY) were housed in the animal facility on a 12 h light/12 h dark cycle with free access to food and water with two rats per cage. All animal procedures were approved by the Uniformed Services University IACUC and complied fully with the principles set forth in the "Guide for the Care and Use of Laboratory Animals" prepared by the Committee on Care and Use of Laboratory Animals of the Institute of Laboratory Resources, National Research Council (DHEW pub. No. (NIH) 85-23, 2985).

Rats were exposed to a moderate controlled cortical impact (CCI) injury over the left parietal cortex as previously described (11). Briefly, rats were anesthetized with isoflurane (4% induction, 2.5% maintenance). Body temperature was maintained at 36.5–37.5ºC by a heating pad that was regulated by a rectal temperature sensor. The animal was placed in a standard rodent stereotaxic frame and positioned using ear and incisor bars. The dorsal scalp was shaved and a mid-sagittal incision was performed under sterile conditions to expose the skull. A 5-mm circular craniectomy was performed over the left parietal cortex at 3.0 mm lateral and 2.0 mm posterior from Bregma. Following the craniectomy, the CCI device (Impact One^{TM}, Leica Microsystems, Buffalo Grove, IL) with a 3-mm flat impactor tip was placed in the center of the craniectomy site and a moderate injury was induced with 5 m/s speed, 200 ms dwell time, and 2 mm deformation depth. Table 1 summarizes the number of rats in each treatment cohort. The skull flap was not replaced after injury and the incision site was closed with surgical staples. Animals were placed in a heated chamber and monitored after injury

until recovery from anesthesia effects and the animal was then returned to their home cage. Sham animals that were used for behavior testing only, received a craniectomy but no CCI intervention and the scalp incision was closed with sutures or staples. For three days post-injury, rats received acetaminophen in the drinking water (200 mg/kg). Table 1 summarizes the number of rats in each treatment cohort, which were utilized for obtaining biosamples for evaluation of insulin treatment after brain injury (left half of table) and behavioral effects (right half of table).

Table 1 – Total numbers of all cohorts -

	Saline Perfused		Fixed		Behavior				Totals
	saline	insulin	saline	insulin	saline	insulin	sham saline	sham insulin	
6hr	5	5	5	5	xxx	xxx	xxx	xxx	20
24hr	5	6	5	4*	xxx	xxx	xxx	xxx	21
4D	5 (4)	6 (4)	5	5	xxx	xxx	xxx	xxx	29
10D	5	5	5**	5**	6	6	3	3	44
28D	xxx	xxx	xxx	xxx	10	10	5	5	30
									144
* one animal died in surgy - not replaced									
**first group (n=3/group) samples destroyed in processing									
() = specifically processed for PCR									

INTRANASAL INSULIN TREATMENT

Under isoflurane anesthesia (4% for induction, 2.5% for maintenance), animals were treated as previously described (11) with intranasal insulin (R-100, Eli Lilly, Indianapolis, IN, 6 IU) or saline (60 µL) beginning 4 h post-injury and continuing with daily administration for 14 days (Fig. 2). They were positioned supine in an anesthesia induction chamber and the treatments were administered by micropipetter into the nasal cavity using 10 µL doses, alternating nares in one minute increments for six doses. After the last dose, the animals remained under anesthesia in the induction chamber for an additional two minutes before being returned to their home cages for recovery. The first treatment was given 4 h after the injury was inflicted (or sham surgery) and then

continued daily through day 14 or until the day of sacrifice, with the exception of the 10-day behavior groups where treatment stopped at day 7. If treatment was administered on the day of sacrifice, it was done two hours prior to tissue collection. For all cohorts, the treatment groups were randomized and each cohort had representatives for all treatment groups. With four or six animals in a surgical cohort, two or three, respectively, would be in each treatment group, selected randomly. For the behavior cohorts, there were six animals per surgical group and they were randomly separated into three groups of two,

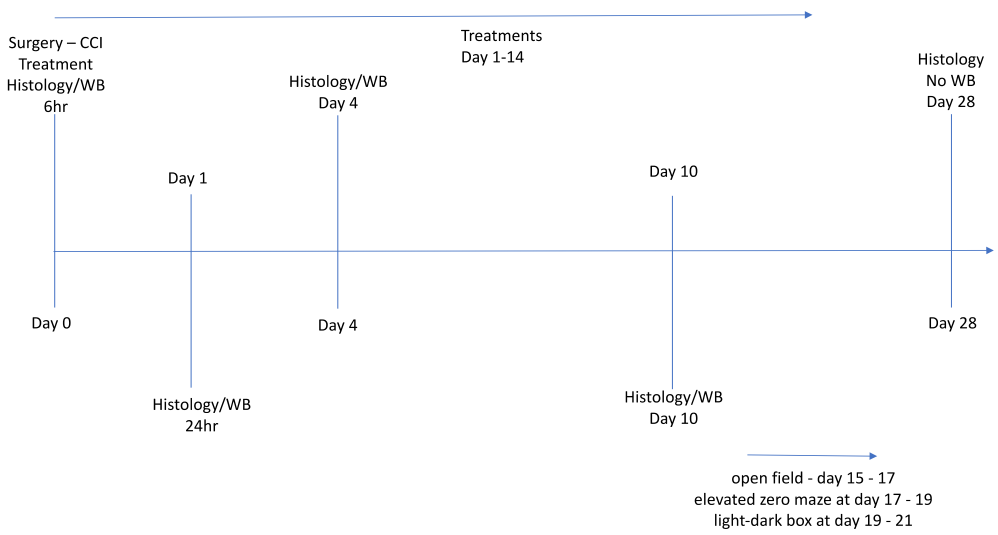

Figure 2. Timeline – visual depiction for timing of treatments, tissue collection, and behavior analysis.

where two animals were treated with saline, two treated with the insulin, and two sham (one treated with saline and one with saline). The selection of all treatment groups was random and the investigator was blinded to treatment.

TISSUE COLLECTION AND PROCESSING

The animals received an intraperitoneal (IP) injection of Euthasol (pentobarbital sodium and phenytoin sodium, Virbac AH, Inc, 0.3 mg/Kg) for deep anesthesia. Fifty

subjects (Table 1) were perfused with saline only and the brains were removed and the cortex surrounding the lesion and the hippocampal area just below it was dissected, immediately frozen, and stored for western blot (WB), enzyme-linked immunosorbent assay (ELISA), and polymerase chain reaction (PCR) procedures as described below.

Thirty-nine subjects (Table 1) were perfused with 10% formalin following the saline perfusion. These brains were removed and sectioned into 20 µm thick slices for histological analysis described below. The sectioning area included a 5 mm tissue block centered on the middle of the lesion after the brain was removed. This 5 mm brain block was frozen in OCT Compound Clear, Optimal Cutting Temperature Embedding Medium for Frozen Tissue Specimens (OCT, Tissue Plus®, Fisher HealthCare, #4585, Scigen Scientific, Gardena, CA) then mounted in the cryostat with the rostral side forward. Every 3rd section was mounted on slides (4 sections per slide) in groups of 10 slides, in a predetermined pattern for Cavalieri method analysis, giving a total of 30 slides (120 mounted slices).

WESTERN BLOT (WB) ANALYSIS

Samples were removed from -80ºC, thawed in ice, and processed as previously described (96) with modifications made for brain tissue. The samples (cortex and hippocampus) were separately processed for protein lysate with RIPA buffer (Pierce™, #89900, Thermo Scientific, Rockford, IL) and protease inhibitors (Halt™, Protease and Phosphatase Inhibitor Single-Use Cocktail, #1861280, Thermo Scientific, Rockford, IL), by adding homogenate solution (RIPA buffer with protease inhibitor) to the tissue based on weight. The resulting solution was then sonicated with 3 second pulses x 3 and then centrifuged at 15000 RPM, 4ºC, for 10 min. The lysate was then pipetted from the

solution and the pellet stored in -80^{o}C. WBs were conducted with 8-12 µg samples per well in Bio-Rad stain-free 15 well (15 µL) gels per factory recommendations. Commercially available antibodies were used to assess signal transduction markers through the MAPK pathway (pMEK1/2, cell signaling #4169, Rabbit, 1:250; MEK1/2, cell signaling #D1A5, Rabbit, 1:500) and the PI3K pathway (pAKT, cell signaling #4060s, Rabbit, 1:250; AKTpan, cell signaling #4691s, Rabbit, 1:500).

ELISA (ENZYME-LINKED IMMUNOSORBENT ASSAY)

ELISA testing used kits purchased from R&D Systems (Minneapolis, MN) for specific cytokines with sample protein concentrations of approximately 25µg/µL. The ELISA kits IL1ß (Rat IL-1 beta/IL-1F2 Quantikine ELISA Kit, RLB00); IL6 (Rat IL-6 Quantikine ELISA Kit, R6000B) and TNFα (Rat TNF-alpha Quantikine ELISA Kit, RTA00) were used to quantitatively assess pro-inflammatory cytokines per manufacturer's instructions.

IMMUNOFLUORESCENCE

The cortex and the CA1 region of the hippocampus (Fig. 3) were assessed for immunohistochemical detection and quantitation of microglia (Iba1, Wako, #019-19741, Rabbit, 1:500) and CD 86 (Cd86, Abcam, #ab53004, Rabbit, 1:200). Neuronal number (NeuN, Millipore, #ABN78, Rabbit, 1:500) and iNOS (iNOS, Abcam, #ab3523, 1:100) were evaluated in the CA1 region of the hippocampus. Samples not stained with primary antibody (negative controls) were used to confirm specificity of secondary used. Quantitation of immunolabeling of was completed using Image J. Two to four images (20x) per subject were captured, converted to 8-bit grayscale images, and the threshold adjusted to where red immunofluorescence on the software's clipboard matched what

was fluorescent in the original image. The new settings were applied and the area of immunolabeling was measured with the recorded averaged for the individual subject. These averages were then used for data analysis.

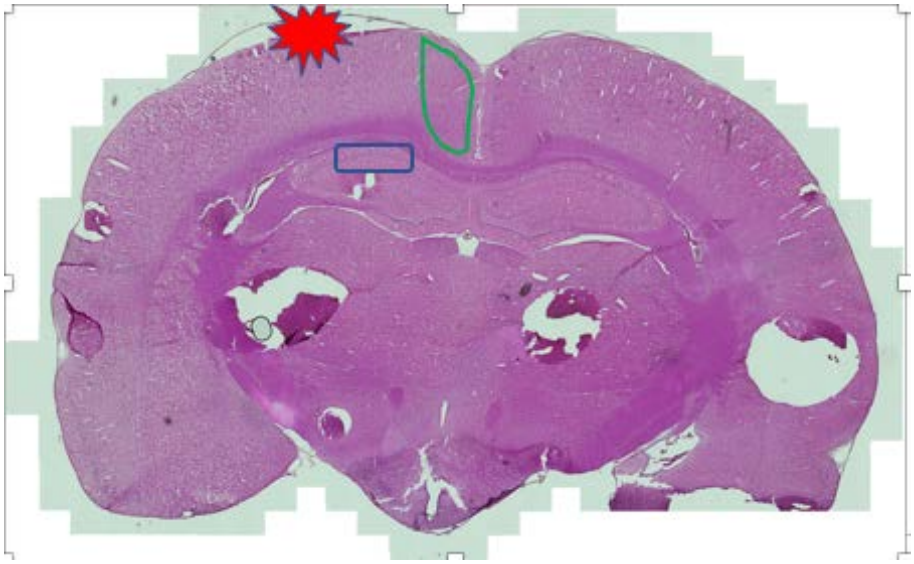

Figure 3. Areas used for analysis in histology. The area of injury (red blast) was the area analyzed with imageJ software to obtain lesion size. The green outlined area was imaged and quantified to analyze cortex for immunofluorescence. The blue outlined area was imaged and quantified for CA1 of hippocampus.

LESION VOLUME

The sections were stained with Haematoxylin and Eosin (H&E) and images of the sections were recorded using Zeiss Axio Scan (5x, Fig. 3). For the lesion analysis, we used slides from three subjects per treatment group, with 3-4 sections averaged per subject as previously described (96). The lesion area of each image was outlined and quantified by an investigator blinded to treatment group with use of ImageJ software. For this analysis, the whole section image (5x) was transferred to the Image J clipboard where the AOI was outlined using the "freehand selection" function. After completing the outline of the AOI, the area of each section was measured and recorded. The Cavalieri method was then used to assess volume for analysis.

BEAM WALKING ASSAY

Animals were trained for three days prior to surgery on a 1 meter beam as previously described (11) with minor modifications. Briefly, rats were trained to walk across a single 2cm thick beam to return to their home cage. For testing, time to cross the beam and number of footfalls were measured at baseline, and at 1, 7, 14 and 21 days post injury by an investigator blinded to treatment group. The animals were tested immediately before treatment as to avoid residual effects of isoflurane exposure.

OPEN FIELD TEST (OFT)

The open field test (OFT) is a measure of general activity levels, gross locomotor activity, exploration, and anxiety (79). Testing for the 28 D cohorts was started after the entire fourteen-day treatment with insulin or saline was completed (Fig. 2 & Table 2). The 10D cohorts started with elevated zero maze two hours after treatment on day seven with no further treatments administered thereafter. The subjects were brought to testing area in home cages for acclimation 30 minutes prior to initiation of testing. A white noise machine (Dohm classic, Marcpac) provided background noise throughout acclimation and testing. The OFT apparatus is an open top, square box (100cm x 100cm x 50cm height) made of gray PVC material. Dimmable track lights mounted on the ceiling illuminated the box to 380 lux. When testing began, the animals were individually placed in the center of the box and allowed to explore for 10 min. At the conclusion, the animal was removed and returned to its cage and the apparatus was cleaned with 70% ethanol before testing the following animal. A ceiling mounted camera connected to a computer recorded the animal's movement using CaptureStar (CleverSys Inc, Reston, VA) and total moving distance, average velocity, center time, center moving

distance and center area entries were analyzed and recorded by the TopScan video tracking software (CleverSys, Inc.).

Table 2 – Behavior testing

28D	15-17 dpi	DPI 17-19	DPI 19-21	DPI 28
	OFT	EZM	LDB	sacrifice
10D	7 dpi	8 dpi	9 dpi	10 dpi
	EZM	OFT	LDB	sacrifice
* OFT - open field test, EZM - elevated zero maze, LDB - light-dark box				

ELEVATED ZERO MAZE (EZM)

The elevated zero maze is used to assess anxiety-related behaviors in rodents (86). The apparatus for this test consists of two closed (with walls) and two open (lacking walls) quadrants on a round maze (diameter 100 cm), elevated 50 cm off the floor (Stoelting Co.). Lighting in the open quadrants was set to 100 lux and 50 lux in the closed quadrants. Time frame for testing is as described in OFT section and (Fig. 2 & Table 2). Each rat was placed in the middle of an open quadrant and allowed to freely explore for 5 min. Between each animal testing, the maze was cleaned with 70% ethanol. The rat's performance was recorded by an overhead camera connected to a computer using the CaptureStar software (CleverSys Inc.). Total moving distance and velocity, time spent in each quadrant, and the number of open quadrant entries was measured using the TopScan video tracking software (CleverSys, Inc.).

LIGHT-DARK BOX (LDB)

The light-dark box test is another behavioral task for evaluating anxiety in rodents(18). The apparatus for this test consists of two compartments, one of which is open and brightly illuminated (800 lux; 40 x 20 x 40 cm) and one which is smaller, dark

and enclosed (0 lux, 40 x 20 x 20 cm), connected through a small opening (10 x 6 cm). Each arena is equipped with photobeam arrays that track the animal in the horizontal and vertical plane. These sensors are connected to the PC with the Fusion 6.4M software (Omnitech Inc.). The software records the number of entries into each box, horizontal and vertical activity, and time spent in both compartments. Time frame for testing is as described in OFT section and (Fig. 2 & Table 2). Animals were placed in the light box and allowed to freely explore for 5 min. The maze was cleaned with 70% ethanol between each animal.

STATISTICAL ANALYSIS

All data were collected by an investigator blinded to treatment group. Lesion volume and ELISA data evaluated using 2-way ANOVA with Tukey's multiple comparisons test. Immunofluorescence and western blot data evaluated using unpaired t-tests using multiple t-test function with correction for multiple comparisons using the Holm-Sidak method with trends over time analyzed via 2-way ANOVA with Tukey's multiple comparisons test. All behavior testing for anxiety evaluated by 2-way ANOVA with Tukey's multiple comparisons test. Beam walk assay not analyzed statistically. All data evaluated and presented via GraphPad Prism 8.

CHAPTER 3: Results - Cellular and Inflammatory Response

Our research design involved adult male Sprague Dawley rats that were exposed to a moderate CCI injury as described in Chapter 2. At 4 hours post-injury, rats received 6IU of Humalog R, or an equivalent volume of saline, based on our previous study (11). Insulin or saline was administered by a pipette in 10µl increments to the rat nasum while the animals were anesthetized with isoflurane. Treatment continued daily for up to 14 days. Brain tissue was extracted for analysis at 6 hours, 24 hours, 4 days, or 10 days post-injury. A total of 90 rats were required for this analysis in immunofluorescence and ELISA (Table 1). Rats were euthanized and brain tissue dissected for immunohistochemical detection and quantitation as well as protein extraction for ELISA analysis (Chapter 2 Methods).

LESION VOLUME IS NOT AFFECTED BY INSULIN TREATMENT

Lesion volume was measured in the affected cortex at 6 hours, 24 hours, 4 days, and 10 days post-injury. Overall, the volume of the lesion appears to start small and then peak at 24hr (Fig. 4). This demonstrates that the injury is not limited to the initial injury but to a progression of continued cell death well after the initial impact. The lesion then gradually resolves over time with the volume returning at 10D to a level similar to that of the 6hr group. With this analysis, it was shown that there is no significant difference in lesion volume between treatment groups at any time point (Fig. 4). This reinforces previous findings and speculation that the decreased IR density in the cortex may have a role in the lack of effect in this area (11).

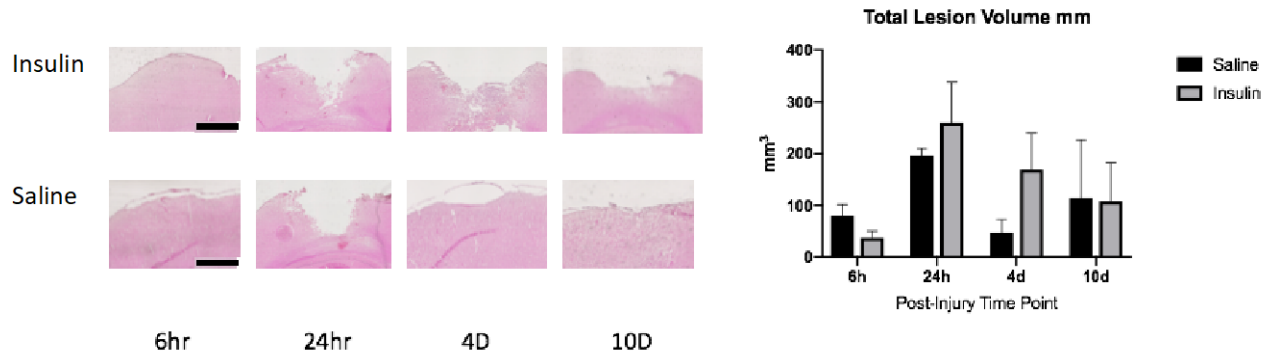

Figure 4. Lesion Volume is not affected by insulin treatment – The lesion starts small and then spikes in volume at 24hrs before gradually declining over time. There is no significant difference between intranasal insulin treated and control at any time point. Representative images of H&E stained cortex at the site of injury. Saline and insulin treated subjects as well as time of sacrifice noted above. The images above were taken from whole section images (Axio Scan, 5x, scale bar = 2.5mm). Lesion volume assessed with ImageJ software by researcher blinded to treatment. n=3/group; bars represent mean +/- SEM.

NeuN in CA1 of the hippocampus

The hippocampus is of chief interest when investigating the mechanism of an improvement in memory with any treatment as the CA1 region of the dorsal hippocampus is directly related to memory (43). Immunofluorescence of the CA1 region with NeuN showed no difference between the treatment groups at any time point but that there is a significant temporal effect (p=0.0136, 2-way ANOVA) and the pixel density appears to be at the lowest point at the 24hr time point. This is in direct contrast to the progression of the lesion volume analysis above (Fig. 4) indicating the injury within the hippocampus is following a similar progression as in the cortex and primarily impacted by secondary injury. Also of note, though there is no difference in pixel density, we do see a difference in morphology within the 4D cohorts (Fig. 5). The 4D control group shows a dispersed arrangement as compared to the compact pattern seen in the insulin

group. This time point coincides with the increased edema volume shown in this area that was significantly decreased by intranasal insulin treatment (11). Though the pixel density does not show a difference, this dispersed pattern might be indicative of increased edema that could have a negative effect on neuronal communication.

IBA1 IS A MARKER OF MICROGLIA/MACROPHAGES

Research has shown that microglia become activated and mobilize to the site of injury after TBI (59). It also shows that at the time of injury, macrophages gain entry into the area and add to the inflammatory process (6; 53). With the methods we are using it is impossible to differentiate between microglia and macrophages as they are both identified by Iba1(59). After probing and evaluating both the cortex and the hippocampus at all time points with Iba1, we can see an expected increase in Iba1 at 4D, in the cortex near the site of injury that is independent of treatment (Fig. 6B, $p=0.0005$, 2-way ANOVA). It is expected because this finding corresponds with what is seen in the literature (59). But we do not see any effect of treatment at any time point.

INTRANASAL INSULIN INDUCES A SIGNIFICANT DECREASE IN PRO-INFLAMMATORY MARKERS

As discussed earlier, microglia, once activated, can take on a pro-inflammatory or anti-inflammatory phenotype. We attempted staining of both phenotypes with use of CD206 (anti-inflammatory), CD86 (pro-inflammatory), and iNOS (pro-inflammatory). We were unable to attain any results from our CD206 immunofluorescence staining (technical difficulties) but did get results with the two pro-inflammatory markers. CD86 is a membrane receptor protein that acts as a co-stimulatory ligand for CD28 that is important for optimal T-cell activation and identifies an antigen presenting cell (in this

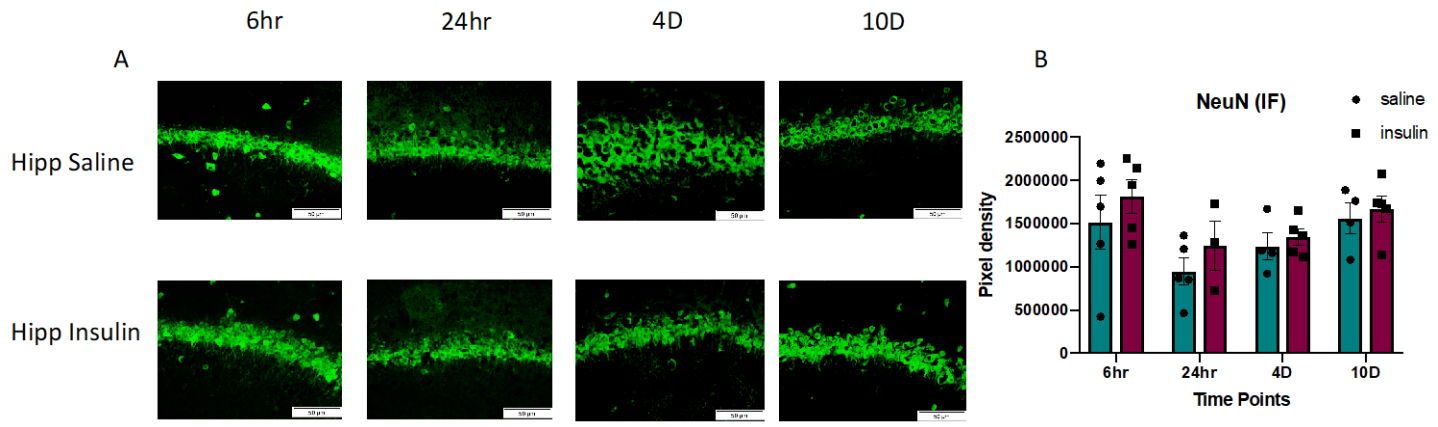

Figure 5. NeuN in CA1 of hippocampus – A) Representative images of CA1 region of hippocampus stained with NeuN. B) Pixel density analysis quantification, bars represent mean +/- SEM and individual data points shown. n = 5-6 per group. X axis = time points, Y axis = pixel density; insulin treated (red bars), control/saline (blue bars). Comparing insulin treated to saline treated control, we see no treatment effect at any time point. After an initial drop at 24hrs, there is a trend to increasing pixel density in both treatment groups. At 4D there is no difference in pixel density quantification but we see a disruption within the neuronal network of the CA1 of the hippocampus in the saline treatment group; a phenomenon we have seen in past studies related to the impact of secondary injury (edema) demonstrated in this area (11).

case a macrophage or microglia) as M1 phenotype (63). Our research shows that when comparing insulin treated to saline treated control after moderate CCI, there is a significant decrease in the insulin treated groups CD86 in both the cortex (p=0.0278) and the hippocampus (p=0.0280) at the acute time point of 6 hours (Fig. 7).

iNOS, also a pro-inflammatory marker of microglial polarization, was also impacted by intranasal insulin (Fig. 8). We show a significant decrease in iNOS at the 4D time point (6hr p=0.3829, 24hr p=0.4683, **4D p=0.0016**, and 10D p=0.4683) with intranasal insulin treatment. Of note, this is also the time of peak microglial activation (Fig. 6). The 10D samples look to suffer from increased variability that might have attributed to the lack of significance therein.

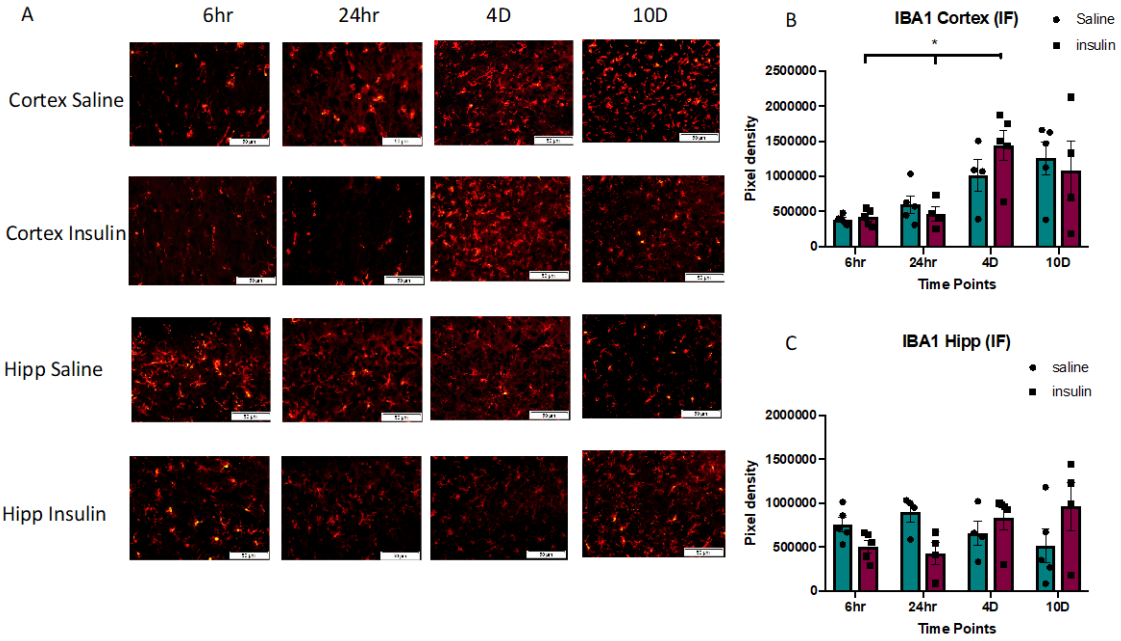

Figure 6. Iba1 a marker of microglia and macrophages, A) Representative images stained with Iba1 of perilesional cortex and CA1 hippocampus treated with either saline or insulin. B-C) Pixel density analysis quantification, bars represent mean +/- SEM and individual data points shown. n = 5-6 per group. X axis = time points, Y axis = pixel density; insulin treated (red bars), control/saline (blue bars). We see no treatment effect at any individual time point. There is a significant increase in overall density in the cortex for insulin treated group from 6hrs and 24hr to 4 days after injury that is independent of treatment. * $p<0.05$, multiple t-tests with Holm-Sidak correction for multiple t-tests, GraphPad Prism 8).

TNFA IS REDUCED WITH INTRANASAL INSULIN TREATMENT

Cytokines are communication proteins that have different effects on different cells depending on the cell type (23). They have a baseline level of activity associated with normal physiology (23). There are pro-inflammatory and anti-inflammatory cytokines that are both active during TBI (21). It is the pro-inflammatory effects that are linked to increased damage after the primary injury and linked with possible options for treatment (13; 21; 46; 53; 68). Our research indicated a significant reduction 24hrs post injury with intranasal insulin treatment (Fig. 9).

TNFα, IL1ß, and IL6 are all pro-inflammatory cytokines associated with TBI. Hippocampal tissue was analyzed and TNFα is significantly reduced at 24hrs post injury

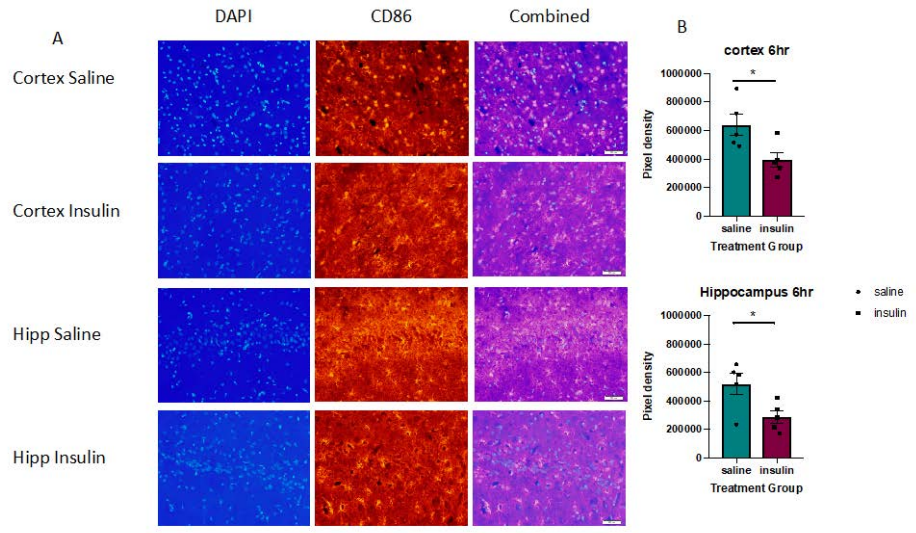

Figure 7. Insulin reduces CD 86 expression at 6 hours. A) Representative images stained with CD86, DAPI, and combined of perilesional cortex and CA1 hippocampus treated with either saline or insulin. B-C) Pixel density analysis quantification, bars represent mean +/- SEM and individual data points shown. n = 5-6 per group. X axis = time points, Y axis = pixel density; insulin treated (red bars), control/saline (blue bars). When comparing insulin treated to saline control, CD86 significantly decreased in the cortex and the hippocampus at 6hrs post injury with intranasal insulin treatment, * $p<0.05$, unpaired t-test.

with intranasal insulin treatment (**24hr p= 0.0336**, 4D p=0.9293, 10D p=0.7331 unpaired t-tests for individual time points) while IL1ß (6hr p=0.9048, 24hr p=0.6232, 4D p=0.9048, 10D p=0.9048) and IL6 (24hr p= 0.8798, 4D p=0.08798, 10D p=0.8798) did not change with treatment. TNFα has been identified as a potentiator of insulin resistance (46) as it blocks insulin receptor signaling via the JNK and NF-□B pathway that inactivate insulin receptor substrate (46). Our research shows that IL6 stays elevated through all three time points tested with no effect of treatment. IL1ß has an initial spike at 6hrs and then drops off to very low levels for the subsequent time points, also showing no effect of treatment.

SUMMARY CHAPTER 3

The data from this chapter follows on the knowledge that TBI causes inflammation in the brain and that insulin decreases that inflammation. We knew that insulin decreased inflammation caused by methamphetamine exposure (7) and that it did

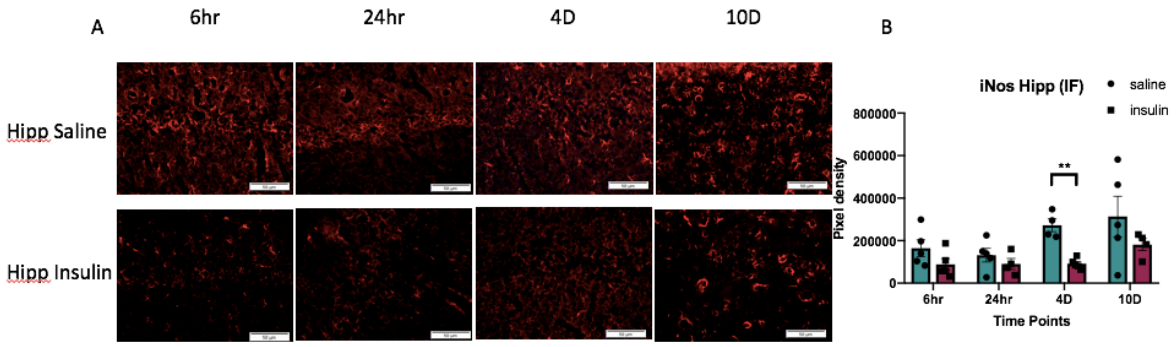

Figure 8. iNOS - a pro-inflammatory marker of microglial polarization, A) Representative images of CA1 region of hippocampus stained with iNOS. B) Pixel density analysis quantification, bars represent mean +/- SEM and individual data points shown. n = 5-6 per group. X axis = time points, Y axis = pixel density; insulin treated (red bars), control/saline (blue bars). When comparing treatment groups in the hippocampus at individual time points iNOS is significantly decreased in the hippocampus at 4D with intranasal insulin treatment. ** p<0.01, multiple t-tests with Holm-Sidak correction for multiple t-tests, GraphPad Prism 8).

affect microglia directly in vitro (10). These data indicate that the decrease in inflammation is not due to a decrease in microglia or macrophages at the site of injury (or on the hippocampus). Instead, it indicates that the effects we see are due to a decrease in pro-inflammatory molecules (i.e. M1 phenotype microglia/macrophages, inflammatory cytokines). Though we were not able to get a direct measurement of the anti-inflammatory players, because there was no change in the number of microglia, it would be a logical deduction that there is an increase in anti-inflammatory agents with insulin treatment. Further testing should be pursued to get direct evidence of this possibility.

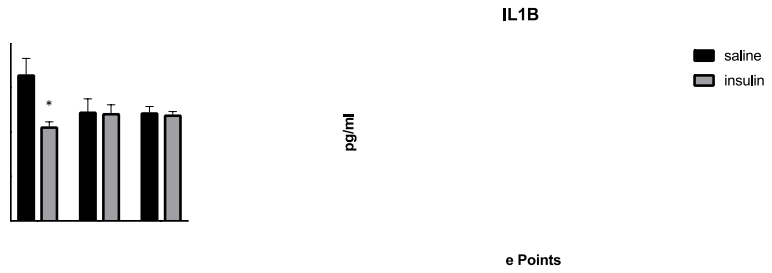

Figure 9. Cytokines - TNFα, IL1ß, and IL6 are all pro-inflammatory cytokines associated with TBI. Hippocampal tissue was analyzed and IL1ß and IL6 show no effects of treatment. TNFα is significantly reduced at 24hrs post injury with intranasal insulin treatment. (SEM, n = 3 per group TNFα & IL6, n = 5 IL1ß, *$p<0.05$, TNFα evaluated with unpaired t-tests for individual time points; IL1ß and IL6 multiple t-tests with Holm-Sidak correction for multiple t-tests, GraphPad Prism 8).

Chapter 4 – Results - Molecular Response

Our previous work indicated that intranasal insulin induced significant effects in the injured hippocampus and on hippocampal related function (11). We attributed the improvement in hippocampal function to high IR concentrations in the hippocampus (105), which can contribute to insulin mediated neuronal survival via PI3K/AKT signal transduction and increased glucose uptake (8; 46). The hippocampus has been directly linked to anxiety (see behavior chapter) (43) and the CA1 region, directly beneath the lesion site, is the most superficial portion of the rat hippocampus (48). The cortex is the actual site of injury but has a reported lower IR density than that of the hippocampus (94). We therefore hypothesized that intranasal insulin would increase intracellular signaling with greater efficacy in the hippocampus than in the cortex through the insulin receptor pathway.

Adult male Sprague Dawley rats were exposed to a moderate CCI injury as described previously (95). At 4 hours post-injury, the rats received 6IU of Humalog R, or an equivalent volume of saline. Insulin or saline was administered by a pipette in 10µl increments to the rat nasum while animals were anesthetized with isoflurane. Treatment continued daily for up to 14 days. Brain tissue was extracted for western blot analysis at 6 hours, 24 hours, 4 days, or 10 days post-injury. A total of 42 rats were required for this analysis (Table 1). Commercially available antibodies were used to assess IR signaling pathways in the cortex and hippocampus. The mechanism was assessed by testing for signal transduction markers through the MAPK pathway and the PI3K pathway. Specifically, we looked for increases or decreases in the phosphorylation of AKT and MAPK.

AKT PHOSPHORYLATION IS NOT AFFECTED BY INSULIN TREATMENT

AKT, also known as protein kinase B, plays a major role in the PI3K/AKT pathway. This pathway is referred to as metabolic and anti-apoptotic because of the major endpoints that include increasing glucose uptake, protein synthesis, lipogenesis, glycogen formation, and blocking apoptosis (Fig. 1). Phosphorylated AKT (pAKT), total AKT (AKTpan), and the ratio of the two (pAKT/AKTpan) was compared between intranasal insulin treated and control (saline) treated groups at each of the 4 time points in the cortex and hippocampus.

In the cortex, when directly comparing insulin treated to control, there was no effect of treatment on pAKT at any time point (Fig. 10B; 6hr p=0.9434, 24hr p=0.9434, 4D p=0.9434, 10D 0; multiple t-tests with Holm-Sidak correction for multiple t-tests). There was also no significant effect on AKTpan was observed between treatment groups (Fig. 10C; 6hr p=0.9776, 24hr p=0.3841, 4D p=0.9776, 10D p=0.9176; multiple t-tests with Holm-Sidak correction for multiple t-tests). As a result, there was no significant effect of treatment was observed on the pAKT/AKTpan ratio (Fig. 10D; 6hr p=0.1250, 24hr p=0.3444, 4D p=0.6696, 10D 0; multiple t-tests with Holm-Sidak correction for multiple t-tests).

Over time in the injured cortex, there is a significant increase in pAKT and pAKT/AKTpan (Fig. 10B) at 4D in the insulin treated groups (6hr to 4D p=0.0086, 24hr to 4D p=0.0003, 2-way ANOVA multiple comparison with Tukey multiple comparison correction). This increase was also seen in the saline treated groups (24hr to 4D p=0.0190, 2-way ANOVA multiple comparison with Tukey multiple comparison correction). There was a spike in expression of AKTpan at 10D that is also independent

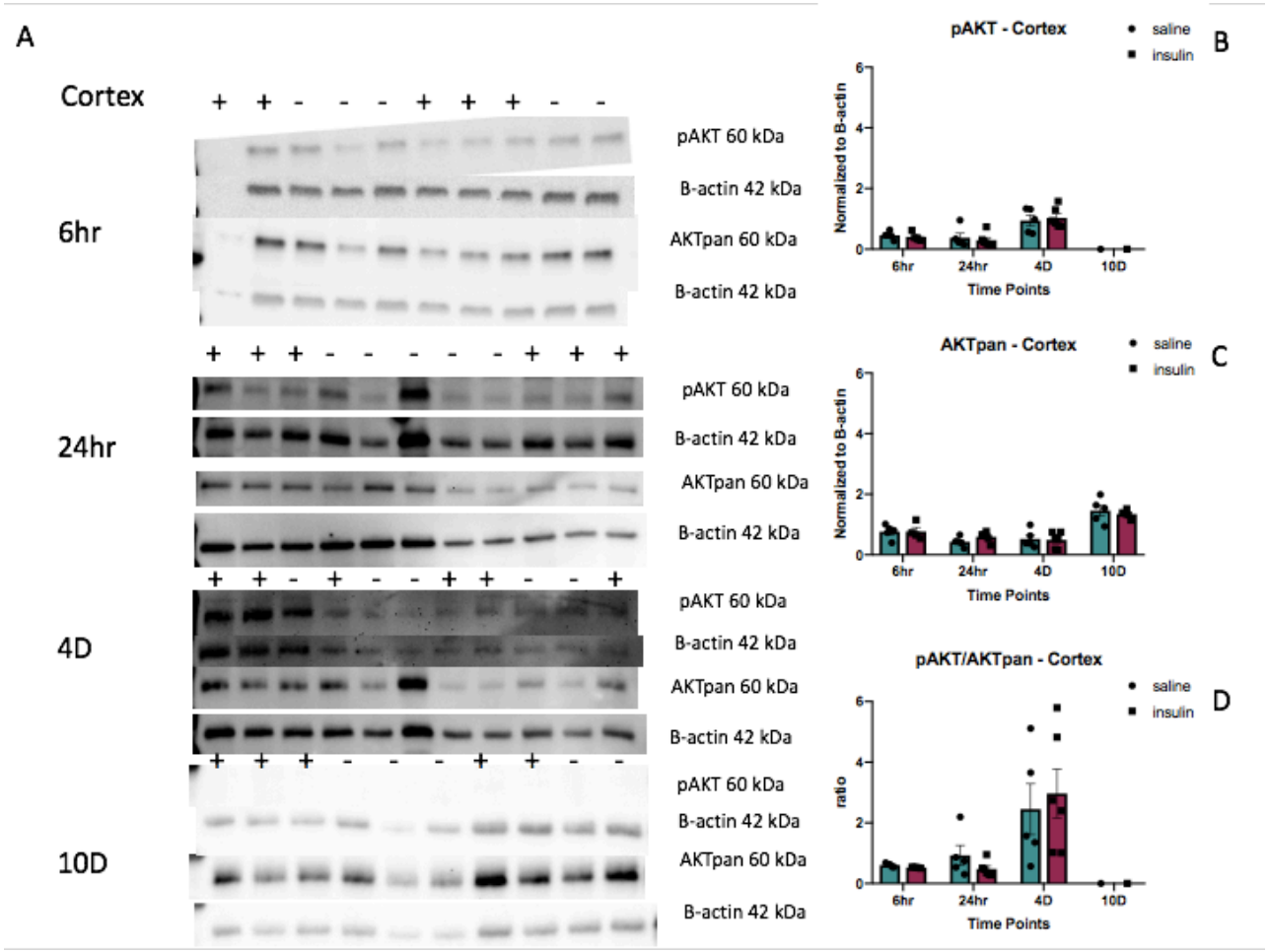

Figure 10 – Insulin has no treatment effect on PI3K/AKT pathway in cortical tissue. A) Scanned images of blots for each time point and treatment (+ insulin, - saline). B) Quantification of pAKT normalized to B-actin. C) Quantification of AKTpan normalized to B-actin. D) Quantification of ratio pAKT/AKTpan after normalization of each. This WB analysis of all four time points shows a temporal effect of TBI with an increase in pAKT/AKTpan at 4D, but there is no difference between the treatment groups at any time point. Bars represent mean +/- SEM and individual data points shown. n = 5-6 per group. pAKT=phosphorylated AKT; AKTpan=total AKT; ratio=pAKT/AKTpan, + insulin treated (red bars), - control/saline (blue bars).

of treatment (Fig. 10C). Within the pAKT/AKTpan ratio (Fig. 10D) analysis, the trend of an increase at 4D returned in the insulin treated groups (6hr to 4D p=0.0196, 24hr to 4D 0.0051, 2-way ANOVA multiple comparison with Tukey multiple comparison correction) and in the saline treated groups (6hr to 4D p=0.1316, 24hr to 4D p=0.3209, 2-way ANOVA multiple comparison with Tukey multiple comparison correction).

In the hippocampus, pAKT (Fig. 11B) shows no significant difference between treatment groups (Fig. 11B; 6hr p=0.6136, 24hr p=0.5820, 4D p=0.6136, 10D p=0.5820; multiple t-tests with Holm-Sidak correction for multiple t-tests). When the time course is compared via 2-way ANOVA, we see a significant drop after 6hrs in the insulin treated groups (Fig 11B; 6hr to 24hr p=0.0331, 6hr to 4D p=0.0094, 6hr to 10D p=0.01112-way ANOVA multiple comparison with Tukey multiple comparison correction) that was not present in the saline treated groups (Fig. 11B; 6hr to 24hr p=0.4053, 6hr to 4D NS p=0.5219, 6hr to 10D NS p=0.1104; 2-way ANOVA multiple comparison with Tukey multiple comparison correction).

AKT pan (Fig. 11C) did not show any significant differences between treatment groups either (Fig. 11C; 6hr p=0.9653, 24hr p=0.9653, 4D p=0.9653, 10D p=0.9653; multiple t-tests with Holm-Sidak correction for multiple t-tests), and showed a similar trend to the pAKT above in that the saline treated groups (6hr to 24hr p=0.3755, 6hr to 4D p=0.0403, 6hr to 10D p=0.9594; 2-way ANOVA multiple comparison with Tukey multiple comparison correction) showed less impact of treatment than the insulin treated (6hr to 24hr p=0.0478, 6hr to 4D p=0.0063, 6hr to 10D p=0.2536, 2-way ANOVA multiple comparison with Tukey multiple comparison correction) before leveling out at 10D.

The ratio of pAKT/AKTpan (Fig. 11D) again gave no significant data for any time point (6hr p=0.7113, 24hr p=0.2680, 4D p=0.2223, 10D p=0.2680; multiple t-tests with Holm-Sidak correction for multiple t-tests) but showed a bimodal trend with an initial drop after 6hr and then a resurgence at 4D. This rendered significant data at different time points but only within the saline treated group (6hr to 10D p=0.0149, 4D to

10D p=0.0024, 2-way ANOVA multiple comparison with Tukey multiple comparison correction).

MEK SHOWS INSULIN TREATMENT EFFECTS

MEK is a kinase involved in the MAPK pathway that is associated with growth and proliferation. As with AKT, phosphorylated MEK (pMEK), total MEK (MEKtot), and the ratio between the two (pMEK/MEKtot) were assessed in both the cortex (Fig. 12) and hippocampus (Fig. 13). pMEK and MEKtot were normalized to vinculin at each time point (SEM, n = 4-5 per group, individual time points evaluated with multiple t-tests with Holm-Sidak correction for multiple t-tests, trends over time done with 2-way

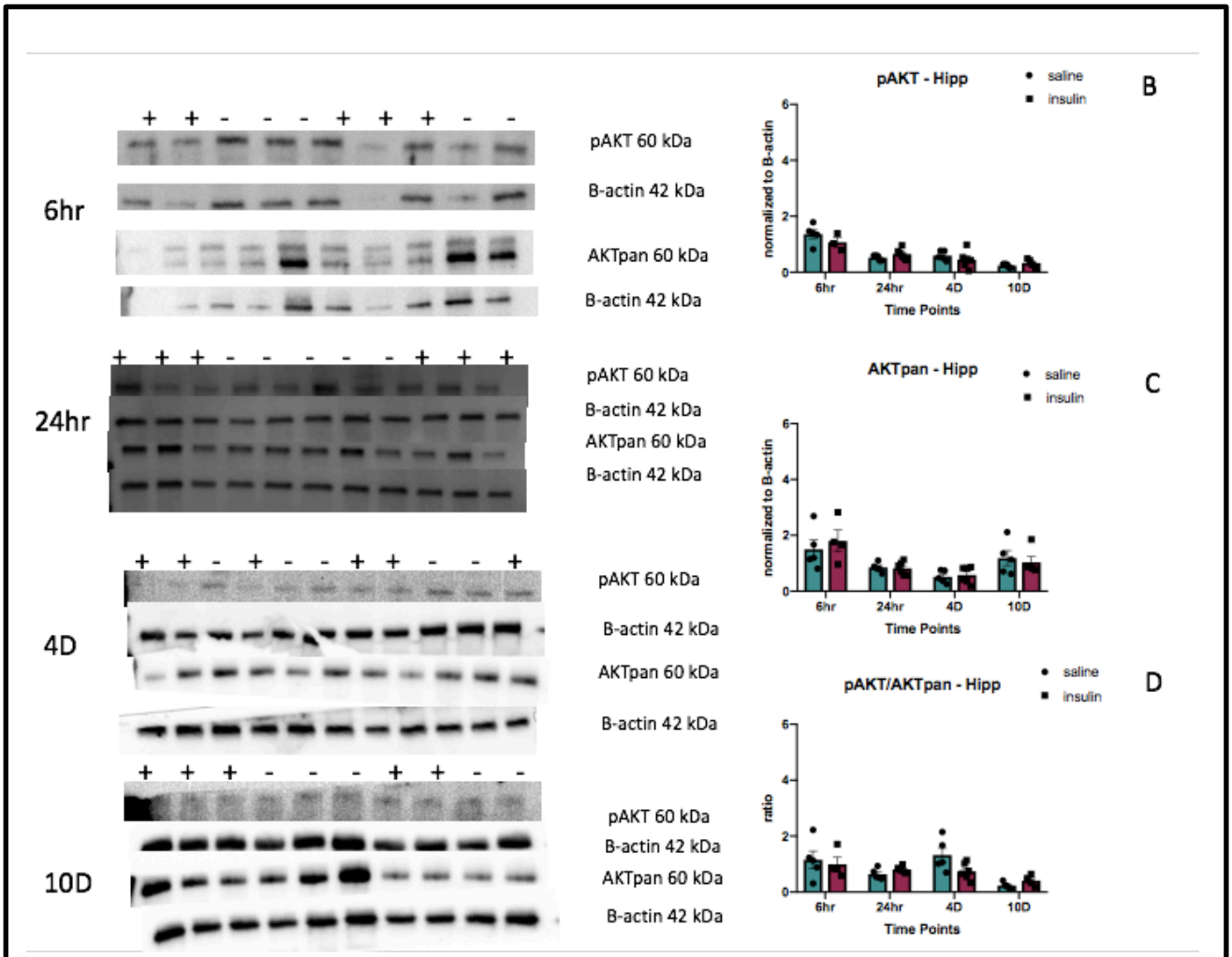

Figure 11. Insulin has potential treatment effect on PI3K/AKT pathway in hippocampal tissue. Intranasal insulin treated vs. control (saline) in each of the 4 time points and considered pAKT, AKTpan and the ratio of the two. A) Scanned images of blots for each time point. B) Quantification of pAKT normalized to B-actin. C) Quantification of AKTpan normalized to B-actin. D) Quantification of ratio pAKT/AKTpan after normalization of each. This WB analysis shows no difference between the treatment groups at any time point. pAKT and AKTpan were normalized to B-actin and each time point. Bars represent mean +/- SEM and individual data points shown. n = 5-6 per group. pAKT=phosphorylated AKT; AKTpan=total AKT; ratio=pAKT/AKTpan, + insulin treated (red bars), - control/saline (blue bars).

ANOVA multiple comparison with Tukey multiple comparison correction). Here, as with AKT, we see a dramatic increase ($p<0.0001$) in phosphorylation of MEK at 4D in the cortex but not in the hippocampus (Fig. 12 & 13). Once again, this corresponds qualitatively with the dramatic increase in Iba1 microglial proliferation (Fig. 6) that was

limited to the cortex. We also see a significant effect of treatment in the cortex at 4D where intranasal insulin appears to increase pMEK/MEKtot compared to saline control.

In the cortex, MEK phosphorylation (Fig. 12B) increases significantly with the 4D treatment groups and continues into the 10D groups. Since this is seen in both the control and insulin treated groups it indicates that the increase in signaling is not dependent on treatment but a factor of time after the injury coinciding with the proliferation of microglia (Fig. 3) in this area. Analysis shows the significant increases in MEK phosphorylation at 4D (saline $p=0.0083$, insulin $p=0.0004$) continued at 10D in the insulin group only (saline $p=0.0680$, insulin $p=0.0009$) when compared to both 6hr and 24hr time points. MEKtot (Fig. 12C) demonstrates no significant differences between treatment groups at any time point (6hr $p=0.6813$, 24hr $p=0.8841$, 4D $p=0.8846$, 10D $p=0.8846$) but a dramatic spike at 10D that is seen in both saline (6hr to 10D $p=0.0002$, 24hr to 10D $p<0.0001$, 4D to 10D $p<0.0001$) and insulin (6hr to 10D $p=0.0006$, 24hr to 10D $p<0.0001$, 4D to 10D $p<0.0001$) with very little variation. We have no explanation for this dramatic increase in MEKtot except that it corresponds with the same phenomenon in AKTpan (Fig. 10C).

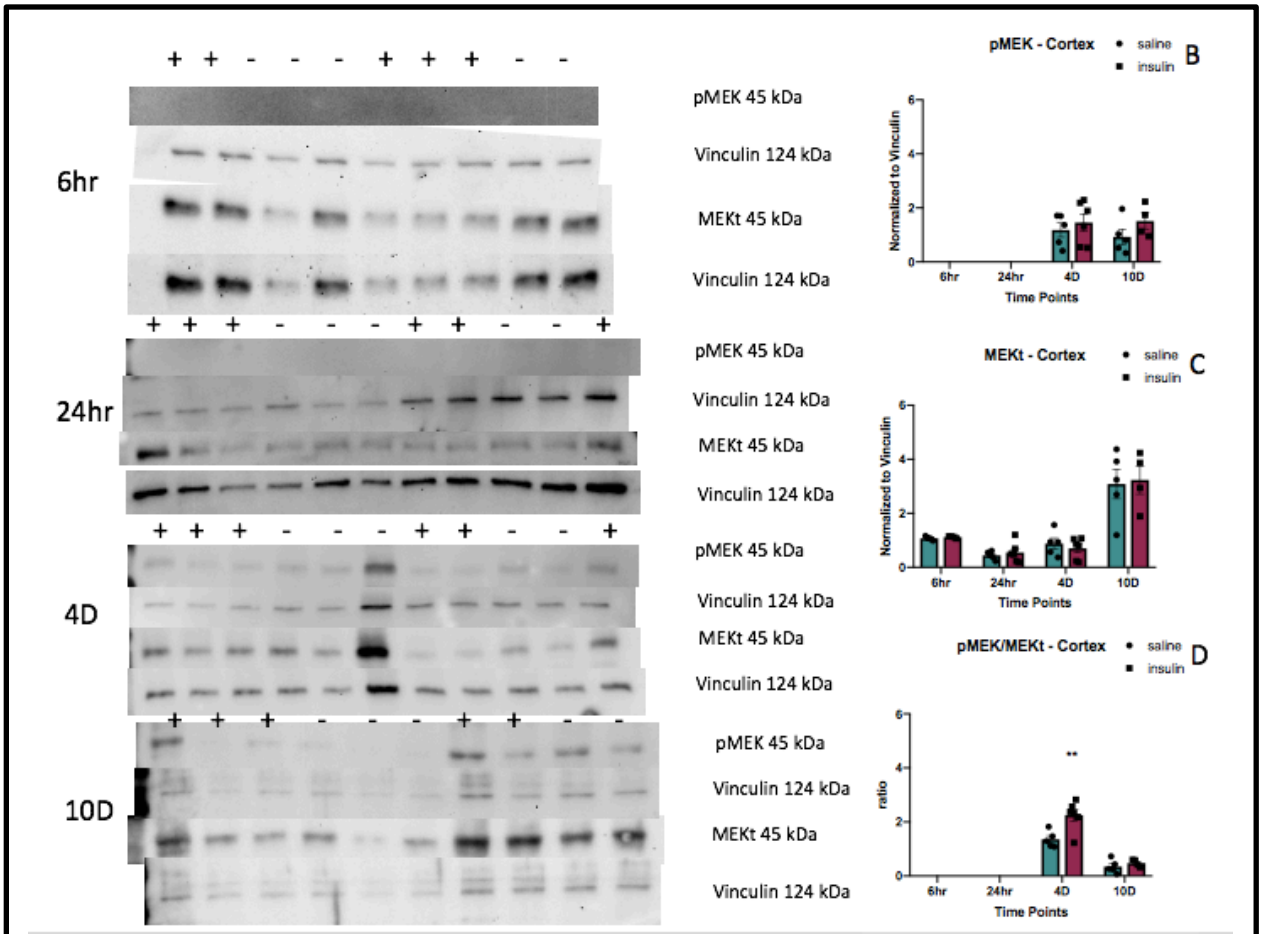

Figure 12. Insulin has a treatment effect on MAPK pathway in cortex tissue. A) Scanned images of blots for each time point. B) Quantification of pMEK normalized to vinculin, 2-way ANOVA analysis shows a significant increase at 4D treatment groups and continues into the 10D groups. C) Quantification of MEKtot normalized to vinculin, demonstrates no significant differences between treatment groups at any time point but a dramatic spike at 10D that is seen in both treatment groups. D) Quantification of ratio pMEK/MEKtot after normalized to vinculin, shows a significant increase at 4D with insulin treatment when compared to control in multiple t-test analysis. 2-way ANOVA shows the significant emergence of activity at 4D in both groups and a significant drop from 4D saline and insulin to the 10D time point. Bars represent mean +/- SEM and individual data points shown (*$p<0.05$). n = 5-6 per group. pMEK=phosphorylated MEK; MEKtot=total MEK; ratio=pMEK/MEKpan, + insulin treated (red bars), - control/saline (blue bars).

pMEK/MEKtot (Fig. 12D) shows a significant increase ($p=0.0203$) at 4D with insulin treatment when compared to control in both multiple t-test analysis. The significant emergence of activity at 4D was seen in both groups ($p<0.0001$) as well as a

significant drop from 4D saline and insulin ($p<0.0001$) to the 10D time point. This drop is undoubtedly influenced by the unexplained spike in total MEK in the 10D groups.

In the hippocampus, pMEK (Fig. 13B) shows no difference between treatment groups at any time point (6hr $p=0.3072$, 24hr $p=0.9150$, 4D $p=0.9150$, 10D $p=0.3755$; multiple t-tests with Holm-Sidak correction for multiple t-tests). Analysis with a 2-way ANOVA shows some differences in the significance of changes between the treatment groups as saline treated groups (6hr to 4D $p=0.0836$, 24hr to 4D $p=0.0003$; 2-way ANOVA multiple comparison with Tukey multiple comparison correction) did not show the same increase at 4D as insulin treated groups (6hr to 4D $p<0.0001$, 24hr to 4D $p<0.0001$; 2-way ANOVA multiple comparison with Tukey multiple comparison correction). Nor did it have as drastic a drop after the 4D time point (saline 4D to 10D $p=0.0061$, insulin 4D to 10D $p<0.0001$; 2-way ANOVA multiple comparison with Tukey multiple comparison correction). This shows a higher level of impact, specifically at the 4D time point, that might be influenced by insulin treatment.

MEKtot (Fig. 13C) shows similar comparison numbers as pMEK in individual time points (6hr $p=0.2550$, 24hr $p=0.9948$, 4D $p=0.6482$, 10D $p=0.2550$; multiple t-tests with Holm-Sidak correction for multiple t-tests). 2-way ANOVA analysis differs from the pMEK trends where now saline treated (6hr to 4D $p>0.9999$, 24hr to 10D $p=0.5902$) shows no changes, while insulin treated (6hr to 4D $p=0.0373$, 24h to 10D $p=0.0451$) has significant changes followed by a drop at 10D with saline (4D to 10D $p=0.3131$) and insulin (4D to 10D $p=0.0007$) that is more dramatic in the insulin treated group.

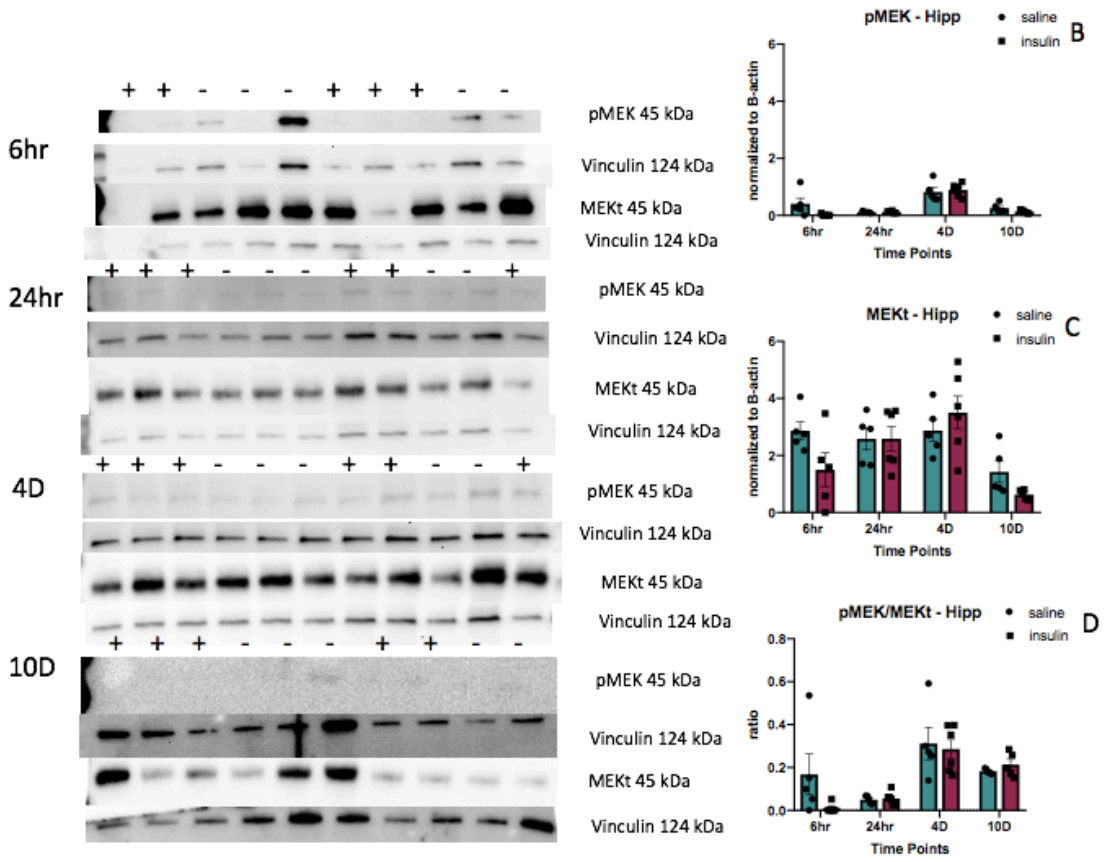

Fig. 13 – Insulin has no treatment effect on MAPK pathway in the hippocampus. A) Scanned images of blots for each time point. B) Quantification of pMEK normalized to vinculin. C) Quantification of MEKtot normalized to vinculin. D) Quantification of ratio normalized to vinculin. This WB analysis of all four time points shows a temporal effect of TBI with an increase in pMEK/MEKtot at 4D, but there is no difference between the treatment groups at any time point. Bars represent mean +/- SEM and individual data points shown. n = 5-6 per group. pMEK=phosphorylated MEK; MEKtot=total MEK; ratio=pMEK/MEKtot, + insulin treated (red bars), - control/saline (blue bars).

The pMEK/MEKtot (Fig. 13D) in the hippocampus, when viewed on the same scale as the other components analyzed, is so small it is difficult to see. For this reason, the scale was altered on this figure only. Here again, there are no differences between treatment groups at any time point (6hr p=0.4511, 24hr p=0.9323, 4D p=0.9323, 10D p=0.6093, multiple t-tests with Holm-Sidak correction for multiple t-tests). The effect over time of saline treated (6hr to 4D p=0.3960, 24hr to 4D p=0.0080) vs insulin treated

(6hr to 4D p=0.0028, 24hr to 4D p=0.0116) shows a greater change within the insulin treated groups.

CONTROLS FOR MEK CONFIRM LACK OF SIGNAL

Two time points in the cortex (6hr and 24hr) showed a lack of signal for pAKT that suddenly appeared at 4D and 10D. In order to confirm this was not due to antibody error, wild type mouse embryonic fibroblasts (MEF) stimulated with epidermal growth factor (EGF) for 5 min (positive control) was processed alongside representative samples from each time point for each treatment group in the cortex and the hippocampus (Fig. 14). The corresponding blot was treated the same as the previous blots for each specific

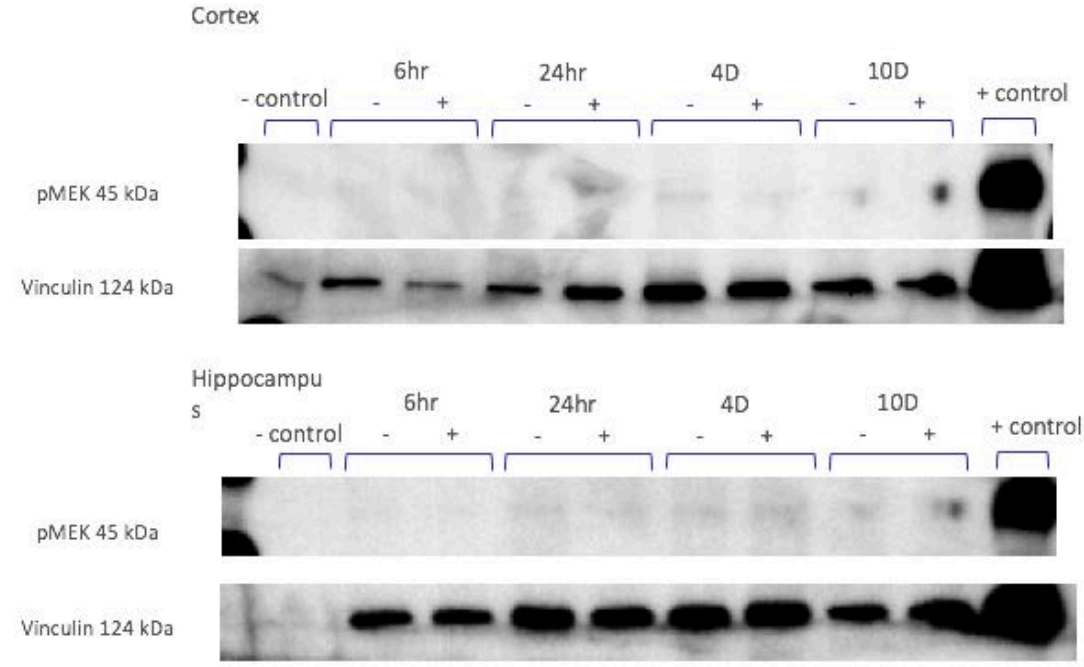

Figure 14. Controls for pMEK. This WB performed to give visual confirmation for the absence of pMEK at time points noted in Figure 11. Bands noted to be absent in the cortex (top) samples for the acute time points (6hr & 24hr) and very light in the hippocampus (bottom) for the same time periods. + control = wild type mouse embryonic fibroblasts (MEF) stimulated with epidermal growth factor (EGF) for 5 min, – control sample buffer only.

time point and confirm that there was no signal at the two acute time points and that the signal appeared and strengthened at 4D and 10D (Fig. 14).

In summary, though these samples were taken from the same animals, the cortex and the hippocampus show distinctly different patterns as to how they respond to CCI injury and intranasal insulin treatment. The cortex shows a dramatic increase in signaling through both PI3K and MAPK pathways at 4D. This phenomenon correlates with the timing of peak accumulation of microglia in this area as seen in chapter 3 (Fig. 6). It is also not reciprocated in the hippocampus where we expected to see a greater impact. Neither the cortex nor the hippocampus show an impact of treatment for AKT at any time point. This is interesting as it is the metabolic pathway and the pathway we expected to be impacted with this treatment. Research has shown that AKT phosphorylation in microglia is increased significantly with insulin treatment when at rest (10). This increase, compared to control, disappears when stimulated by lipopolysaccharide (LPS), found on the outer membrane of gram-negative bacteria. In this model, we are stimulating both treatment groups with TBI and therefore might be negating the effects. MEK does show an impact of treatment at the 4D time point in the cortex. The increase in MEK phosphorylation at 4D with injury makes sense as it is associated with increased growth and proliferation and this time point corresponds with the increase in Iba1 in this area. But the increase in phosphorylated MEK does not correlate with an increase in Iba1 begging the question as to what this increase is influencing. There is research that indicates that MEK might have an impact in microglial/macrophage polarization, an area we did see significant changes, that will be discussed in chapter 6.

Chapter 5 – Results – Behavior

TBI affects the limbic system with evidence of impact from injury to the hippocampus (11) and psychiatric impairments including anxiety (62; 91). Intranasal insulin has shown a significant effect on the progression of injury and memory, which is also associated with this area of the brain (11; 37). Intranasal insulin has also been shown to alleviate methamphetamine induced anxiety and neuroinflammation (7) but to this point, behavioral analyses for TBI have not included anxiety.

We hypothesized that intranasal insulin administration following moderate TBI would reduce anxiety-like symptoms. We proposed to test this hypothesis utilizing the open field test (OFT), elevated zero maze (EZM), and light-dark box (LDB) following moderate TBI and insulin administration.

Adult male Sprague Dawley rats (see Table 1 for numbers) were exposed to a moderate controlled cortical impact (CCI) injury as described previously (95) for two experimental designs (28D and 10D). At 4 hours post-injury, all rats received 6IU of Humalog R, or an equivalent volume of saline. Insulin or saline was administered by a pipette in 10µl increments to the rat nasum while animals are anesthetized with isoflurane. Treatment was continued daily through day 14 for 28D groups and through day 7 for the 10D groups. Treatments done on day of testing were performed >2 hours prior to testing to decrease the influence of anesthesia on behavior.

A total of 48 rats were used (Table 1) and testing occurred between 0900 and 1100. When testing began, the animals were placed in the middle of the light/open chamber facing away from safety and then released. The animals were undisturbed and videotaped for 5-10 minutes based on individual protocol.

Open field (OFT): Although the OFT is primarily used to measure locomotor activity, it can also evaluate anxiety and in some cases, depression (1; 17; 49). Anxiety is measured by the amount of time the animal explores the center area (17; 49). Typically, the animal will initially stay near the walls until it becomes familiar with the chamber. As it acclimates, a normal animal will begin to explore the center area, but an anxious animal will continue to hug the sides of the chamber (17).

Elevated zero maze (EZM): The zero maze was created as a modification of the elevated plus maze (EPM) (14; 62). Similar to the EPM, the EZM has been used for antianxiety drug effectiveness testing and therefore demonstrated face and predictive validity (17; 97). The maze is constructed of a circular track elevated approximately a meter from the floor. The track is divided into four quadrants of equal length. Opposing quadrants have sides that are closed and the two others are open. The animal will feel safer within the closed areas as the sides provide "protection". So, like in the EPM when the researcher places the animal in the middle of an open area, the animal will initially find its way into one of the closed quadrants (17). Once it has explored both of the closed arms, animals will normally explore the open arms. Increased open arm activity (duration and/or entries) reflects decreased anxiety-like behavior (97).

Light-dark box (LDB): The LDB is another test that is employed for measuring anxiety-like behavior in rodents (31). The apparatus has two compartments and an opening (door) connecting them. The "light" side consists of a larger portion of the overall space and is a transparent, well illuminated structure. The "dark" side is completely enclosed to include a non-transparent lid. Normal animals will prefer the dark area but will have a tendency to explore when placed in a novel environment. The

anxious animal will remain in the dark protected area with no significant presence in the light (31).

INSULIN REDUCES TIME TO CROSS BUT NOT FOOT FALLS ON BEAM WALK

The beam walk assay was performed to test both motor and cognitive symptoms. The simple task of walking across the beam gives an indicator that the animal can perform behavior assessments without motor dysfunction being a confounding factor. This data replicates previous results from the same injury/treatment paradigm (11). For this reason, we limited the data collection to one cohort. Footfall assessment confirmed that animal motor function is intact and that the impact of injury impacted the right hind

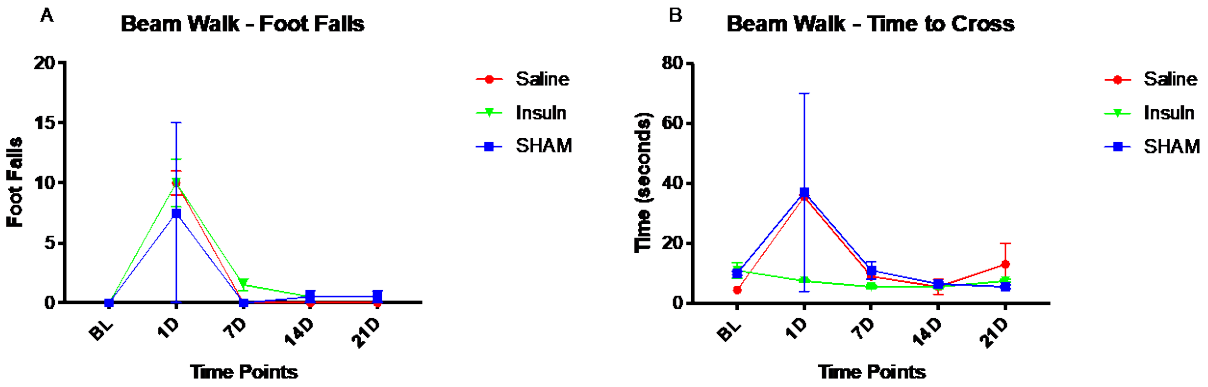

Figure 15 - Beam Walk – Data replicates previous results from same injury/treatment paradigm(11). (A) Footfall assessment confirms animals motor function is intact and that impact of injury limited to right hind limb with transient dysfunction. The impact of injury resolves prior to time of behavior testing independent of injury or treatment group. (B) Crossing time shows insulin treated animals performing better than both injured control and sham. SEM, n=2/group.

limb with transient impairment (Fig. 15A). The impact of injury resolves prior to the time of behavior testing independent of injury or treatment group. Though the sample size is too small to quantify, the time taken to cross shows a similar pattern as our previous research (11), where it was shown that there was a difference between treatment groups at 24hours that resolved prior to one week (Fig.15B).

NO INJURY OR TREATMENT EFFECT ON ANXIETY-LIKE BEHAVIOR FOR 28 DAY COHORTS

The 30 animals used for the 28-day study were broken into cohorts of 6 and all subjects were randomized within all groups. These cohorts were further broken down to represent all of the treatment and injury options (i.e. 2 CCI with saline treatment, 2 CCI with insulin treatment, 1 sham with saline treatment, and 1 sham with insulin treatment). The animals were selected and labeled randomly and prior to initiation of any surgical procedures. After 14 days of treatment, OFT (Fig. 16A; Total distance p=0.1587, velocity p=0.1587, center time p=0.9182, center entries p=0.1490; 2-way ANOVA multiple comparison with Tukey multiple comparison correction), EZM (Fig. 16B; distance p=0.9413, velocity p=0.7508, open area time p=0.9779, open area entries p=0.7888; 2-way ANOVA multiple comparison with Tukey multiple comparison correction), and LDB (Fig. 16C; time in light area p= 0.5223, entries into light area p= 0.3585; 2-way ANOVA multiple comparison with Tukey multiple comparison correction) show no significant statistical interaction. They also show no visual patterns of an increase in anxiety-like behavior after CCI compared to sham. This is interesting as we know that anxiety is a common result of TBI in humans (62; 91). We speculate that the lack of injury effect might be associated with the fact that both treatment groups (saline vs insulin) also received isoflurane for anesthesia. Isoflurane is both neuroprotective and even being investigated as a potential treatment for depression (99).

NO INJURY OR TREATMENT EFFECT ON ANXIETY-LIKE BEHAVIOR AT 7, 8, OR 9 DAYS POST-INJURY

Because our preliminary results (not shown) showed an impact of injury and treatment on hyperactivity (seen as an indicator of anxiety (62)) with the EZM, we chose to construct a new study around the parameters of those preliminary results. The preliminary testing was done on a cohort of one of the 10D groups and was done on day 7, greater than 2hrs after that day's treatment. This shorter timeline would also decrease the amount of time the animals were receiving isoflurane. Therefore, this new study was started with the same CCI procedure as all other cohorts with the same treatment protocol. The 18 animals used for this study were again broken into groups of 6 with representatives of all injury and treatment options (i.e. 2 CCI with saline treatment, 2 CCI with insulin treatment, 1 sham with saline treatment, and 1 sham with insulin treatment).

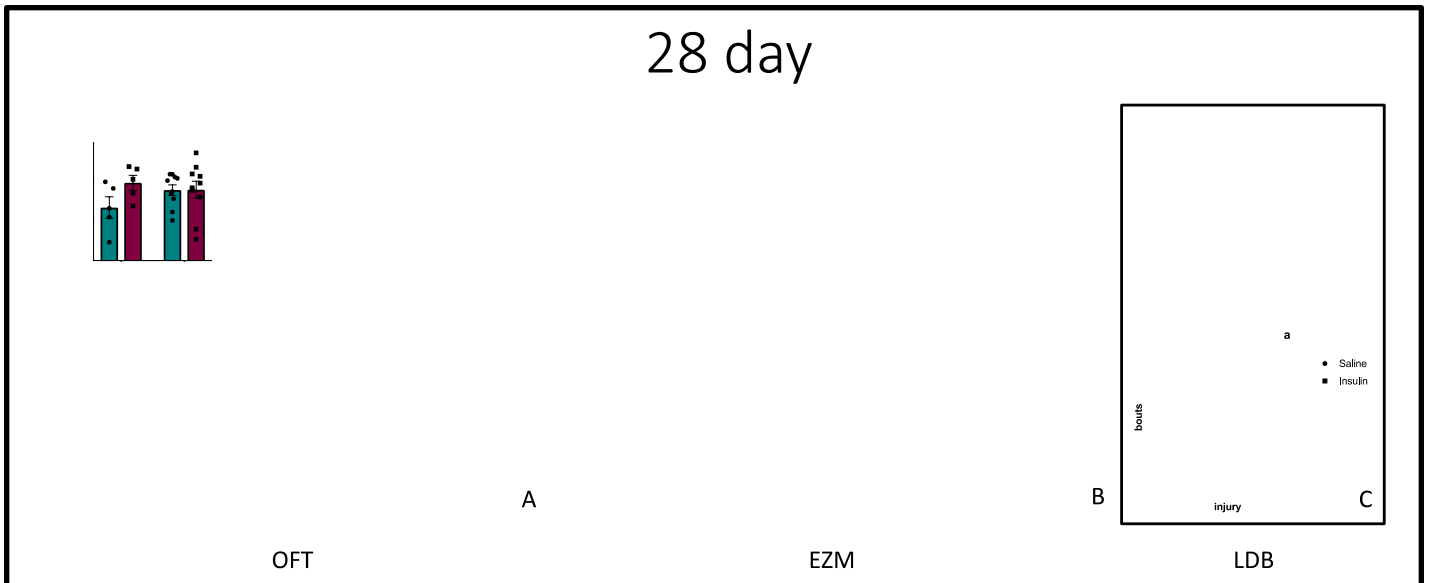

Figure 16 - No injury effect after 14 days of treatment - With the 28D cohorts, the animals received all 14 days of treatment prior to the initiation of testing (table 2 & 4). OFT (A) – total distance, velocity, center time, center entries showed no difference of injury or treatment. EZM (B) total distance, velocity, open area time, open area entries showed no difference of injury or treatment. LDB (C) time in light area, entries into light area showed no difference of injury or treatment. Bars represent mean +/- SEM, n = 5 sham saline, 5 sham insulin, 10 CCI saline, 10 sham insulin.

At day 7, treatment was performed and the behavior testing (EZM) performed greater than two hours later. There were no further treatments and the subsequent tests were administered over the next two days (OFT day 8, LDB day 9). The results from this new study showed no significant effect of injury or treatment on any measure of anxiety-like behavior (OFT: Fig. 17A, total distance p=0.5346, velocity p=0.2875, center time p=0.0.0365, center entries p=0.2983; EZM: Fig. 17B, open area time p=0.8435, open area entries p=0.5314; and LDB: Fig. 17C, time in light area p= 0.4373, entries into light area p= 0.0162; 2-way ANOVA multiple comparison with Tukey multiple comparison correction).

Though we were looking for an impact of intranasal insulin on anxiety, this was predicated on the previous research that showed TBI and CCI induce anxiety.

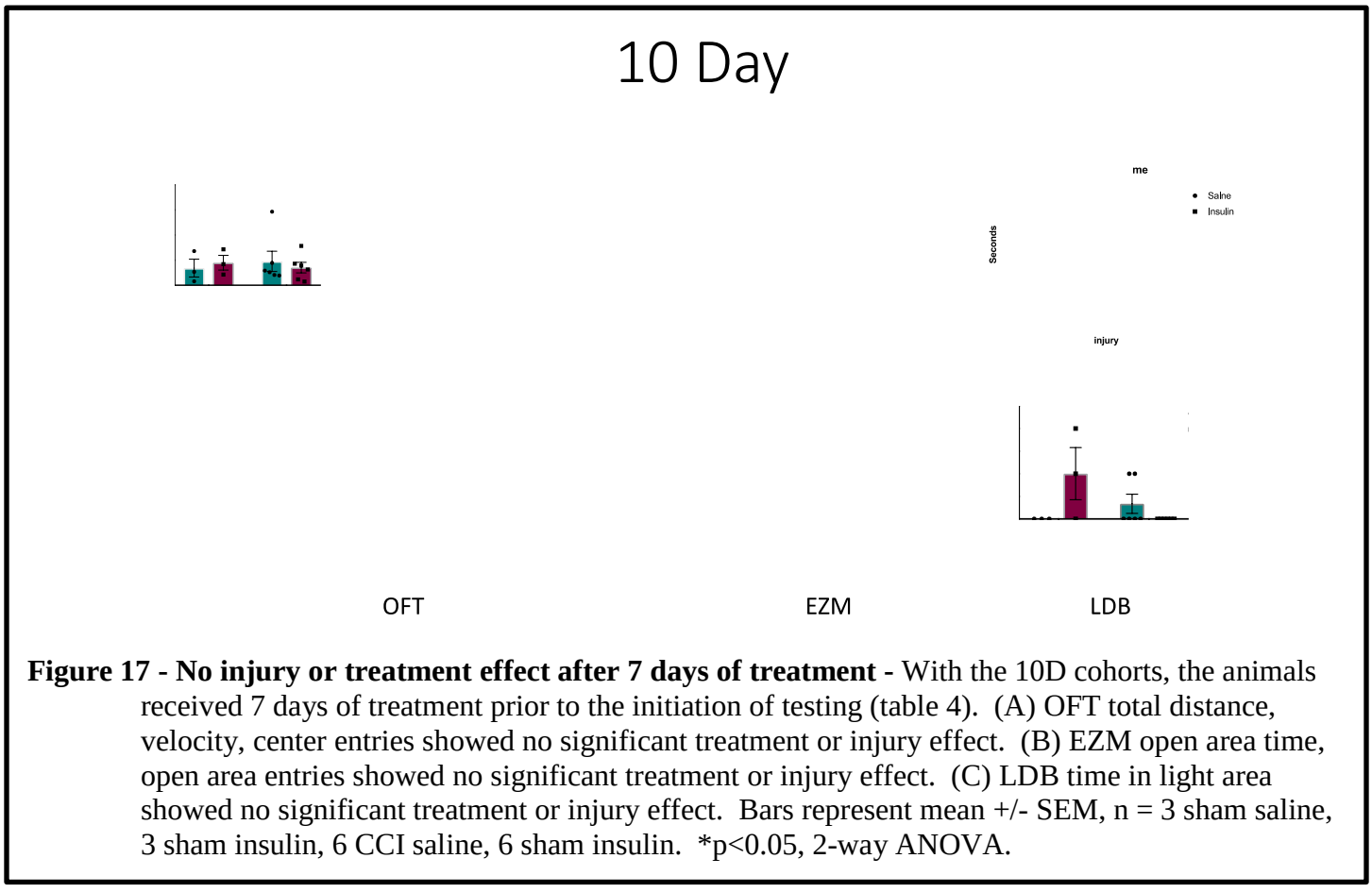

Figure 17 - No injury or treatment effect after 7 days of treatment - With the 10D cohorts, the animals received 7 days of treatment prior to the initiation of testing (table 4). (A) OFT total distance, velocity, center entries showed no significant treatment or injury effect. (B) EZM open area time, open area entries showed no significant treatment or injury effect. (C) LDB time in light area showed no significant treatment or injury effect. Bars represent mean +/- SEM, n = 3 sham saline, 3 sham insulin, 6 CCI saline, 6 sham insulin. *p<0.05, 2-way ANOVA.

Unfortunately, this study did not show that there was an increase in anxiety-like behavior after CCI and therefore, could not evaluate intranasal insulin as a treatment.

Chapter 6 – Discussion

This study provides important information about how intranasal insulin affects the brain after TBI. These data contribute to the body of knowledge elaborating on the efficacy of intranasal insulin as a therapy for TBI, as well as the mechanism for how it achieves that efficacy. Currently, there is no effective treatment for the deficits that develop after TBI. Establishing an effective treatment is complicated by gaining access to the central nervous system (CNS) because of the protection from the blood-brain barrier (BBB). Our previous work demonstrated that after a moderate TBI in rats, intranasal insulin administered within 4 hours after injury significantly increased glucose uptake in the hippocampus, improved cognitive function, and reduced inflammation (11). However, the mechanism by which insulin has these effects and the temporal course of these effects was currently unclear. The goal of this study was to determine if intranasal insulin administration would reduce inflammation and neuronal loss in the hippocampus and reduce measures of anxiety in rats exposed to moderate TBI. We also wanted to evaluate the mechanism by which intranasal insulin administration affects the hippocampus and potentially improves memory function to broaden its therapeutic potential for treatment of TBI in a rat model. To accomplish these goals, adult male Sprague Dawley rats were exposed to a moderate controlled cortical impact (CCI) injury. Intranasal insulin treatments were administered 4 hours after injury and then daily for 14 days. Histological analysis with NeuN was used to assess total number of neurons in the hippocampus. In order to assess inflammation, microglial/macrophage density and activation in the hippocampus were measured as well as the production of cytokines. Also, multiple behavior tests, including open field, elevated zero maze and light-dark

box, were used to assess anxiety. Overall, we found that intranasal insulin did not have a significant effect on neuronal (NeuN, Fig. 5) or microglial/macrophage (Iba1, Fig. 6) density, but did decrease expression of CD86 (Fig. 7), iNOS (Fig. 8), and TNFα (Fig. 9) within the hippocampus. Cellular signaling demonstrated that intranasal insulin increased the phosphorylation of MEK in the cortex (Fig. 12), but no signal transduction pathway alterations were noted in the hippocampus (Fig. 13). With this model, TBI did not increase anxiety-like behavior when compared to sham-treated animals (Fig. 16, 17), negating the ability to evaluate treatment. Therefore, overall these data are inconclusive, but do suggest a transient suppression of pro-inflammatory molecules in the acute post-injury period through an undetermined mechanism of action.

Chapter 3 emphasized the role that inflammation plays in the secondary process of TBI and replicates the progress of microglial/macrophage response to the point of injury that has been shown in the literature (59). This chapter also shows that intranasal insulin has an effect on pro-inflammatory signals as it decreases CD86, iNOS, and TNFα. Chapter 4 looked at the cell signaling involved after the administration of intranasal insulin. It was found that there was a treatment effect of insulin via the MAPK pathway (pMEK/MEKtot) at the 4D time point and not at all through the PI3K pathway (AKT). Chapter 5 demonstrated that with this model, TBI did not alter anxiety-like behavior after TBI.

INTRANASAL INSULIN HAD LITTLE EFFECT AT CELLULAR LEVEL

Our previous data indicated that intranasal insulin had significant effects on the injured hippocampus and hippocampal related function (11). We attributed the improvement in hippocampal function to high IR concentrations in the hippocampus

(105), which contributes to insulin mediated neuronal survival via increased glucose uptake and PI3K/AKT or MAPK signal transduction (signaling discussed in chapter 4). Based on this, we hypothesized that intranasal insulin would reduce neuronal damage in the CA1 region of the hippocampus (Fig. 3), which is directly beneath the lesion site, is the most superficial portion of the rat hippocampus (48) and is associated with memory (43).

We also hypothesized that treatment with intranasal insulin would decrease inflammation after TBI. Microglia are the resident macrophage-like cells of the brain and serve an important purpose in the acute stages following TBI that include clearing cellular debris (21; 35; 59; 82). However, it has been shown that prolonged classical activation (M1) can be detrimental due to the release of pro-inflammatory cytokines, nitric oxide, and reactive oxygen species that can result in neuronal cell death (59). We have demonstrated that insulin reduces microglial number at 21 days after a moderate TBI (11). Also, insulin has been shown to significantly reduce pro-inflammatory cytokines and iNOS expression in vitro (10). However, it is unclear if the observed improvements in hippocampal related function is occurring as a result of neuronal changes, inflammatory changes, or if one leads to the other. Therefore, we hypothesized that intranasal insulin treatment would decrease inflammation after TBI and reduce neuronal damage in the CA1 region of the hippocampus.

The time points for evaluation were derived from the cascade of events that proceed over time following moderate TBI. There are different dynamic changes going on throughout the acute, subacute, and chronic time points after injury, all of which may play into secondary injury. These changes include the initial spike, then decrease

followed by general resurgence of glucose uptake (11). At the same time, there is the initial spike of pro-inflammatory mediators, then the surge of anti-inflammatory cytokines, followed by the peak of microglial accumulation (59). Because of all these dynamic changes over time, we chose to perform histological evaluation at acute (6, 24 hours), sub-acute (4, 10 days) and chronic (28 days) time points. The 28 day cohorts are the animals that participated in the first of the anxiety experiments discussed in Chapter 5. These animals were sacrificed and the tissue was collected but not processed or evaluated as part of this dissertation due to time constraints. It will be evaluated as part of a future project.

First, we looked to the area of impact in the brain and the volume of the resultant lesion. To evaluate the effect of intranasal insulin on lesion volume in the cortex after CCI, we performed H&E stains on tissue from each time point with representatives from animals treated with insulin or saline. Previous research did not show a significant impact of intranasal insulin on the area of impact (11). The speculation is that this might have to do with a lower IR density in the cortex compared to some other parts of the brain (i.e. the hippocampus) (11). Then neuronal (NeuN) and microglial (Iba1) number in the cortex and CA1 region of the hippocampus (Fig. 5 & 6) were assessed using pixel density analysis. Because of difficulty locating a consistent area for analysis, neuronal density was only assessed in the hippocampus (Fig. 5). But Iba1 was imaged and quantified in both the cortex and CA1 of the hippocampus (Fig. 6). In addition to these cellular assessments, commercially available antibodies against the M2/anti-inflammatory markers CD206, and M1/pro-inflammatory markers CD86, and iNOS were used to assess pro- and anti-inflammatory activation of microglia in the same regions. CD206 was not

completed due to technical problems. CD86 was used to assess both the cortex and the hippocampus, but due to discontinuation of the antibody, we were only able to assess the 6hr cohort. We ran into the same issues with iNOS that we had with NeuN and again were limited to just the hippocampus. Tissue was also harvested and protein extracted for ELISA (Chapter 2). The ELISA was performed on hippocampal tissue only and per manufacturers direction to quantitatively assess the pro- and anti-inflammatory cytokines IL1ß, IL6, TNFα, and IL10 within the hippocampal region. For TNFα, 6hr samples were not evaluated due to lack of sample at the time the test was run. IL1ß and IL6 were run at a later time and 6 hour tissue was available. The IL10 ELISA was scrapped due to error during processing.

Lesion volume showed no effect of insulin treatment at any time point. The slope of increase and then subsequent decrease in lesion volume mirrors the slope we see of NeuN immunofluorescence in the hippocampus giving credence to the progression of the injury in both the cortex and the hippocampus. Decrease in NeuN immunofluresence should not be seen as a loss of neurons, but can be interpreted as an impact of injury that can return as neurons recover (93). NeuN in the hippocampus did not show a quantitative difference between treatment groups at any time point, but there is a qualitative observation in the 4D groups. We see in the control group that there is a dispersed pattern that is not present in any of the other images. This could be caused by the increased edema we have shown through previous MR imaging (10). It is possible that this organizational disruption is having an effect on the neuronal transmission within the area.

Ionized calcium binding adaptor molecule 1 (Iba1) is a protein that is specifically expressed in microglia and macrophages (41; 71). It peaks, independent of treatment, in the cortex at 4D in our studies which matches what is demonstrated in the literature (59). This was expected as it is the time where not only the microglia converge on the site of injury, but also the peak of macrophage entry with the disruption of the BBB (40; 59). It is interesting that though there was a significant increase in Iba1 density in the cortex over time, we did not see any effect of treatment in this area. It was thought that decreasing inflammation would induce a decrease in microglial/macrophage density. This does not appear to be the case.

PRO-INFLAMMATORY AGENTS APPEAR SUSCEPTIBLE TO INTRANASAL INSULIN TREATMENT

Though the density of Iba1 was not affected by insulin treatment, it would appear that the phenotype of macrophages/microglia in the area is. CD86 and iNOS are associated with classically activated microglia (M1 polarization). Our data show that there is a significant decrease in CD86 and iNOS expression with insulin administration. The decrease in CD86 with treatment was seen in both the cortex and the hippocampus at 6 hours. This is earlier than expected as the peak of microglial activity is closer to 4D.

Inducible nitric oxide synthase (iNOS) belongs to the nitric oxide synthase (NOS) family of enzymes that catalyzes the production of nitric oxide (NO), which plays a key role in the pathogenesis of inflammation (52). iNOS was also affected by insulin treatment, showing a significant decrease in immunofluorescence in the 4D time points in the hippocampus. Though it does coincide with the time point where we saw the most microglial activity, that significant increase in activity was in the cortex only. There was no increase in Iba1 density in the hippocampus, suggesting that insulin has an effect on

polarization that is independent of proliferation. It has been previously shown *in vitro* that insulin has a direct effect on microglia by decreasing NO, ROS, and cytokines (10). These data demonstrate a similar effect of insulin *in vivo*.

Tumor necrosis factor alpha (TNFα) is a pro-inflammatory cytokine produced by macrophages, microglia, and astrocytes and a key player in neuroinflammation (26; 76). It is associated with the acute phase of inflammation and has also been reported as having a link to insulin resistance through JNK and NF-kB pathways (46). Neuroinflammation and insulin resistance have been linked to increased morbidity in TBI as well as other disease processes like rheumatoid arthritis, bowel disease, and Alzheimer's disease (26; 76; 89). Insulin has been shown to decrease TNFα release from BV2 microglia in vitro after being stimulated by lipopolysaccharide (LPS) (10). This data suggests an in vivo translation and a potential implication for this potential therapy.

INTRANASAL INSULIN ADMINISTRATION HAD A GREATER EFFECT ON THE GROWTH PATHWAY THAN METABOLIC

Our previous work indicated that intranasal insulin induced significant effects in the injured hippocampus and on hippocampal-related function (11). We attributed the improvement in hippocampal function to high IR concentrations in the hippocampus (105), which can contribute to insulin mediated neuronal survival via PI3K/AKT signal transduction and increased glucose uptake (8; 46). We therefore hypothesized that intranasal insulin would increase intracellular signaling with greater efficacy in the hippocampus than in the cortex through the insulin receptor pathway.

Our data show that there is a greater level of phosphorylation of both pathways within the cortex at the 4D time point that is independent of treatment. Further, only the phosphorylation of MEK in the 4D cohorts shows an effect of treatment, with a

significant increase in phosphorylation of MEK in the insulin group (Fig. 12). This would indicate that this model shows a greater impact on growth and proliferation via MAPK than metabolism or anti-apoptosis via the PI3K/AKT pathway. Previous research in BV2 microglia demonstrated that the addition of insulin increased AKT phosphorylation in unstimulated microglia indicating that the PI3K pathway is the pathway activated by insulin treatment (10). But this study went on to also show that this increase in AKT phosphorylation was present in both treatment groups, independent of the addition of insulin, when stimulated by LPS (10). These previous results, combined with this current research, would suggest that the PI3K pathway is not the primary signaling pathway when microglia are stimulated with insulin. It would also suggest that if these results reflect changes to the microglia, as they only constitute 15% of the cellular makeup, are quite diluted in their presentation. The contrast might be much stronger if separated out from other cell types for further examination.

There is also some discussion as to the effect of MEK on the polarization of microglia. A recent study does indicate that inhibition of the MAPK pathway inhibits M1 polarization and promotes the M2 phenotype (104). This is interesting in that our data indicates that intranasal insulin treatment causes a decrease in iNOS (pro-inflammatory marker) at the same time point that the treatment stimulates an increase in MEK (MAPK pathway) phosphorylation. It would seem that these are in contradiction, but we must consider that with the protein extraction process we used there is no way to ascertain what cells are showing this increased activity.

ISOFLURANE COULD BE A CONFOUNDING FACTOR IN ANXIETY TESTING

TBI can induce anxiety in both humans and in rodents (7; 50) but the evaluation of anxiety-like behavior has been questioned (91). Though there are questions as to the validity of anxiety testing rodents and the translation to actual human emotion (31; 62), testing for anxiety-like behavior has proven useful in the investigation of the effects of medication for anxiety (32). Based on this knowledge, we planned behavior testing for anxiety-like behavior to compare insulin to saline treated animals.

First, we started with the beam walk assay to confirm there were no changes in motor skills. Injury to the motor cortex in the injury could impair the animal's performance. We did note that all the animals were able to perform the task at least one week after injury (Fig. 15). The anxiety testing was predicated on preliminary data that showed a lot of promise. We found that there was a significant difference between the treatment groups showing an increase in hyperactivity (sign of anxiety) without the treatment (data not shown). We performed a power analysis based on these data and what was in the literature and planned the testing to follow the full two weeks of treatment as outlined in our previous studies (11). What we found was that there was a large amount of variability within each of the groups in all of the time points.

After completing the planned study with 30 animals it was seen that there was no effect of injury. This is to say that our data was not showing that TBI increase anxiety-like behavior in these subjects. We then paused and reviewed the design, making note that isoflurane is neuroprotective and was being investigated as a treatment for depression. It is possible that since both treatment groups were receiving isoflurane that it could be negating the effects of TBI and therefore negating our study into the treatment of TBI induced anxiety. So, to minimize the exposure to isoflurane and follow up on the

positive data we had previously collected, we decided to attempt to mirror the preliminary experiment more closely. We therefore moved the testing times back to day 7 and ran another study. Unfortunately, again, we did not get any significant results.

As mentioned above, the numbers for these experiments was assessed to be low after a more specific power analysis could be done. This was especially true in the sham group as there were half as many sham animals in each of the treatment groups. Also, the literature does point out that the testing of anxiety in rodents is difficult and ambiguous as it is testing anxiety-like behavior and might be the reason for the large variability (31; 62; 91).

There is a need to consider what constitutes a "sham" when it comes to comparison for behavioral analysis. In some forms of TBI research, simply exposing an animal to anesthesia is considered sham. This is really all that can be done for things like CHIMERA (closed-head impact model of engineered rotational acceleration) which involves a closed head injury and therefore no surgery to expose to. But contrast this with what is done for CCI. For CCI sham, we not only exposed the animal to anesthesia and a surgical incision to the scalp, we performed an actual craniectomy. The literature is clear that the performance of a craniotomy/craniectomy cannot be done without causing some damage to the underlying tissue (24; 72). Efforts can and are made and precautions taken to minimize the damage, but it cannot be totally eliminated. That being said, it is necessary for the use of as specific of a sham as possible to minimize the factors that can be considered when evaluating the data. For this reason, it may be advisable to include different levels of sham into the equation. For our study, this might include naïve, naïve with anesthesia only, anesthesia with ear pins and scalp incision, as well as craniectomy.

With some of these other options, we cannot only look at the injury itself, but also if the surgical injury from craniectomy is playing a role in the results.

STUDY LIMITATIONS

In all of our studies the goal was to analyze both the cortex and the hippocampus. But tissue processing proved to cause some problems with this goal for some of the experiments, especially with the immunofluorescence. NeuN was not analyzed in the cortex related to difficulty determining a specific site to evaluate consistently with issues like lesion volume size changes over time and tissue easily damaged and/or folded in the injured area. Pixel density was used to compare insulin treated to control due to limited time of the investigator, but for more detailed results to assess neuronal viability, counting neurons with stereology would be more effective.

One of our key objectives was to evaluate pro-inflammatory and anti-inflammatory molecules (polarization markers, cytokines). We did attempt evaluation of CD86, CD206, YM1, Arg1, iNOS, IL1ß, IL6, IL10, and TNFα. For various reasons discussed below, we were not able to assess all of these markers/cytokines, in both the cortex and hippocampus, in all time points with the modalities we were using (WB, immunofluorescence, ELISA).

CD86 showed significant differences between treatment groups in the first time point tested (6hr) in both the cortex and the hippocampus. Unfortunately, we are unable to see if this significance plays out in any other time point (Fig. 7). The reason for the limited testing was a discontinuation of the antibody by the distributor prior to the completion of our study. This does show a promising area of research and should be continued when the antibody becomes available again.

We did try to test the anti-apoptotic possibility through cleaved caspase 3 testing via western blot and immunofluorescence but were unsuccessful in getting an antibody response to either the treated or the control animal. It would be beneficial in a future study to separate out the independent cell types. This has been done in cell culture and could be done *in vivo* using flow cytometry to examine which cell types are being affected by the treatment.

One of the complications we noted with the testing we performed for cell signaling was that the samples were a mix of cells and we cannot differentiate which cells were demonstrating the signaling we were seeing. It was clear that we did see a clear increase in the phosphorylation of both PI3K (AKT) and MAPK (MEK) pathways at 4D that was independent of treatment. We also saw an increase in Iba1 at that same time point. But this could lead to many different possible conclusions. It could be that the increase in MAPK pathway reflects an increase in growth and proliferation of the microglial cells that are mobilizing to the area of injury. With this same theory, the increase in PI3K (metabolic pathway) could indicate that these same microglial cells are very metabolically active. Another possibility is that the PI3K pathway (also known as anti-apoptotic) is more active in cells trying to survive the secondary cascade and inflammatory response they are being exposed to. This attempt at survival could be through the increased metabolic needs of a threatened and/or damaged cell, or it could be through direct action of anti-apoptosis.

CONCLUSIONS AND FUTURE DIRECTIONS

The data adds to the body of knowledge as to the mechanism of the effect of intranasal insulin after TBI. And though it falls short on giving therapeutic insight for the treatment of anxiety, it does bring up ideas for how to change the research paradigm in order to better evaluate this potential therapy in future experiments. Intranasal insulin clearly decreases pro-inflammatory molecules that have been shown to cause pathogenesis. This has been demonstrated in both *in vitro* and *in vivo* work and could be the cause of the positive results that are being seen with this therapy. This study also gives more insight into the therapeutic window for the treatment. Our lab has considered and evaluated, in conjunction with this study, different timing and dosing to add to the body of knowledge of when is the best time to treat.

As noted above, we did attempt to test other pro-inflammatory markers, as well as several anti-inflammatory markers, but many were unsuccessful. We postulated that this might be due to low protein expression or post-translational modifications so our lab is using quantitative PCR to determine alteration in mRNA transcript levels as a function of injury and insulin treatment.

We also note that with this model, intranasal insulin has an effect on the MAPK pathway through increased phosphorylation of MEK. As this coincides with the increase in growth and proliferation of microglia, future investigation should be done in individual (i.e. neurons, microglia, astrocytes, etc.). As noted above, insulin treatment of stimulated microglia has been performed in vitro with BV2 (an immortalized microglial cell line) cells (10).

Anxiety continues to be a huge problem after TBI in humans, and though this testing did not reveal any new information into a potential treatment, it should continue to

be investigated. As noted above, we suspect that isoflurane plays a role in the ineffectual data we have collected so far and have been working out a plan to eliminate it as a variable in this research. Our lab has started performing intranasal insulin treatments without isoflurane to remove that variable from the equation. With several days of training to include gentle contact and intranasal saline, the animals have become tolerant of the therapy and can then receive either intranasal insulin or saline control after CNS injury without anesthesia. We should also consider the inclusion of additional control groups, including a treatment group that does not receive a craniectomy. This will increase the numbers required for testing but will give more validity to the results.

Insulin has been around for decades to treat diabetes, a manageable disease that people died of not that long ago. This research suggests that, when given intranasally to rodents after moderate CCI, it decreases some pro-inflammatory molecules at specific time points. And previous research has shown that it improves memory after moderate CCI without the negative side effects of decreased blood sugar or body weight. As this is a simple and adaptable treatment model that could be implemented at the point of injury, continued research is needed to evaluate its benefits in the treatment of TBI.

REFERENCES

1. Abdul Shukkoor MS, Baharuldin MT, Mat Jais AM, Mohamad Moklas MA, Fakurazi S. 2016. Antidepressant-Like Effect of Lipid Extract of Channa striatus in Chronic Unpredictable Mild Stress Model of Depression in Rats. *Evid Based Complement Alternat Med* 2016:2986090
2. Alvarez JI, Katayama T, Prat A. 2013. Glial influence on the blood brain barrier. *Glia* 61:1939-58
3. Andriessen TM, Jacobs B, Vos PE. 2010. Clinical characteristics and pathophysiological mechanisms of focal and diffuse traumatic brain injury. *J Cell Mol Med* 14:2381-92
4. Archer T. 2012. Influence of physical exercise on traumatic brain injury deficits: scaffolding effect. *Neurotox Res* 21:418-34
5. Ariza M, Serra-Grabulosa JM, Junque C, Ramirez B, Mataro M, et al. 2006. Hippocampal head atrophy after traumatic brain injury. *Neuropsychologia* 44:1956-61
6. Batchelor PE, Tan S, Wills TE, Porritt MJ, Howells DW. 2008. Comparison of inflammation in the brain and spinal cord following mechanical injury. *J Neurotrauma* 25:1217-25
7. Beirami E, Oryan S, Seyedhosseini Tamijani SM, Ahmadiani A, Dargahi L. 2017. Intranasal insulin treatment alleviates methamphetamine induced anxiety-like behavior and neuroinflammation. *Neurosci Lett* 660:122-9
8. Blazquez E, Velazquez E, Hurtado-Carneiro V, Ruiz-Albusac JM. 2014. Insulin in the brain: its pathophysiological implications for States related with central insulin resistance, type 2 diabetes and Alzheimer's disease. *Front Endocrinol (Lausanne)* 5:161
9. Bohringer A, Schwabe L, Richter S, Schachinger H. 2008. Intranasal insulin attenuates the hypothalamic-pituitary-adrenal axis response to psychosocial stress. *Psychoneuroendocrinology* 33:1394-400
10. Brabazon F, Bermudez S, Shaughness M, Khayrullina G, Byrnes KR. 2018. The effects of insulin on the inflammatory activity of BV2 microglia. *PLoS One* 13:e0201878
11. Brabazon F, Wilson CM, Jaiswal S, Reed J, Frey WHN, Byrnes KR. 2017. Intranasal insulin treatment of an experimental model of moderate traumatic brain injury. *J Cereb Blood Flow Metab* 37:3203-18
12. Brabazon F, Wilson CM, Shukla DK, Mathur S, Jaiswal S, et al. 2017. [(18)F]FDG-PET Combined with MRI Elucidates the Pathophysiology of Traumatic Brain Injury in Rats. *J Neurotrauma* 34:1074-85
13. Bramlett HM, Dietrich WD. 2007. Progressive damage after brain and spinal cord injury: pathomechanisms and treatment strategies. In *Neurotrauma: New Insights into Pathology and Treatment*:125-41. Number of 125-41 pp.
14. Braun AA, Skelton MR, Vorhees CV, Williams MT. 2011. Comparison of the elevated plus and elevated zero mazes in treated and untreated male Sprague-Dawley rats: effects of anxiolytic and anxiogenic agents. *Pharmacol Biochem Behav* 97:406-15

15. Byrnes KR, Wilson CM, Brabazon F, von Leden R, Jurgens JS, et al. 2014. FDG-PET imaging in mild traumatic brain injury: a critical review. *Front Neuroenergetics* 5:13
16. Carson MJ, Doose JM, Melchior B, Schmid CD, Ploix CC. 2006. CNS immune privilege: hiding in plain sight. *Immunol Rev* 213:48-65
17. Carter M, Shieh J. 2010. Chapter 2 - Animal Behavior. In *Guide to Research Techniques in Neuroscience*:39-71: Academic Press. Number of 39-71 pp.
18. Chaouloff F, Durand M, Mormede P. 1997. Anxiety- and activity-related effects of diazepam and chlordiazepoxide in the rat light/dark and dark/light tests. *Behav Brain Res* 85:27-35
19. Chapman CD, Frey WH, Craft S, Danielyan L, Hallschmid M, et al. 2012. Intranasal Treatment of Central Nervous System Dysfunction in Humans. *Pharmaceutical Research* 30:2475-84
20. Chauhan NB, Gatto R, Chauhan MB. 2010. Neuroanatomical correlation of behavioral deficits in the CCI model of TBI. *J Neurosci Methods* 190:1-9
21. Chen Z, Trapp BD. 2016. Microglia and neuroprotection. *J Neurochem* 136 Suppl 1:10-7
22. Cherry JD, Olschowka JA, O'Banion MK. 2014. Neuroinflammation and M2 microglia: the good, the bad, and the inflamed. *J Neuroinflammation* 11:98
23. Christman JW, Wheeler AP, Bernard GR. 1991. Cytokines and sepsis: What are the therapeutic implications? *Journal of Critical Care* 6:172-82
24. Cole JT, Yarnell A, Kean WS, Gold E, Lewis B, et al. 2011. Craniotomy: true sham for traumatic brain injury, or a sham of a sham? *J Neurotrauma* 28:359-69
25. Davidson RJ. 2002. Anxiety and affective style: role of prefrontal cortex and amygdala. *Biol Psychiatry* 51:68-80
26. DiSabato DJ, Quan N, Godbout JP. 2016. Neuroinflammation: the devil is in the details. *Journal of Neurochemistry* 139:136-53
27. Dixon CE, Clifton GL, Lighthall JW, Yaghmai AA, Hayes RL. 1991. A controlled cortical impact model of traumatic brain injury in the rat. *J Neurosci Methods* 39:253-62
28. Donatti AF, Soriano RN, Leite-Panissi CR, Branco LG, de Souza AS. 2017. Anxiolytic-like effect of hydrogen sulfide (H2S) in rats exposed and re-exposed to the elevated plus-maze and open field tests. *Neurosci Lett* 642:77-85
29. Dyrna F, Hanske S, Krueger M, Bechmann I. 2013. The blood-brain barrier. *J Neuroimmune Pharmacol* 8:763-73
30. Edbladh M, Fex-Svenningsen Å, Ekström PAR, Edström A. 1994. Insulin and IGF-II, but not IGF-I, stimulate the in vitro regeneration of adult frog sciatic sensory axons. *Brain Research* 641:76-82
31. Ennaceur A. 2014. Tests of unconditioned anxiety - pitfalls and disappointments. *Physiol Behav* 135:55-71
32. Ennaceur A, Michalikova S, van Rensburg R, Chazot PL. 2010. Distinguishing anxiolysis and hyperactivity in an open space behavioral test. *Behav Brain Res* 207:84-98
33. for Neuroscience S. 2018. Brain Facts. *The Society for Neuroscience*

34. Fridman EA, Beattie BJ, Broft A, Laureys S, Schiff ND. 2014. Regional cerebral metabolic patterns demonstrate the role of anterior forebrain mesocircuit dysfunction in the severely injured brain. *Proc Natl Acad Sci U S A* 111:6473-8
35. Fung TC, Olson CA, Hsiao EY. 2017. Interactions between the microbiota, immune and nervous systems in health and disease. *Nat Neurosci* 20:145-55
36. Giza CC, Hovda DA. 2014. The new neurometabolic cascade of concussion. *Neurosurgery* 75 Suppl 4:S24-33
37. Hanson LR, Frey WH, 2nd. 2008. Intranasal delivery bypasses the blood-brain barrier to target therapeutic agents to the central nervous system and treat neurodegenerative disease. *BMC Neurosci* 9 Suppl 3:S5
38. Harris JJ, Jolivet R, Attwell D. 2012. Synaptic energy use and supply. *Neuron* 75:762-77
39. Herman JP, Ostrander MM, Mueller NK, Figueiredo H. 2005. Limbic system mechanisms of stress regulation: hypothalamo-pituitary-adrenocortical axis. *Prog Neuropsychopharmacol Biol Psychiatry* 29:1201-13
40. Hsieh CL, Kim CC, Ryba BE, Niemi EC, Bando JK, et al. 2013. Traumatic brain injury induces macrophage subsets in the brain. *Eur J Immunol* 43:2010-22
41. Ito D, Imai Y, Ohsawa K, Nakajima K, Fukuuchi Y, Kohsaka S. 1998. Microglia-specific localisation of a novel calcium binding protein, Iba1. *Brain Res Mol Brain Res* 57:1-9
42. jenny apelt gm. 1999. Insulin-Sensitive GLUT4 Glucose Transporters Are Colocalized With GLUT3-Expressing Cells and Demonstrate a Chemically Distinct Neuron-Specific Localization in Rat Brain. *Journal of Neuroscience Research* 57:693-705
43. Jimenez JC, Su K, Goldberg AR, Luna VM, Biane JS, et al. 2018. Anxiety Cells in a Hippocampal-Hypothalamic Circuit. *Neuron* 97:670-83 e6
44. Jorge RE, Acion L, Starkstein SE, Magnotta V. 2007. Hippocampal volume and mood disorders after traumatic brain injury. *Biol Psychiatry* 62:332-8
45. Kalsbeek MJ, Mulder L, Yi CX. 2016. Microglia energy metabolism in metabolic disorder. *Mol Cell Endocrinol* 438:27-35
46. Karelina K, Weil ZM. 2016. Neuroenergetics of traumatic brain injury. *Concussion* 1:CNC9
47. Khajavikhan J, Vasigh A, Kokhazade T, Khani A. 2016. Association between Hyperglycaemia with Neurological Outcomes Following Severe Head Trauma. *J Clin Diagn Res* 10:PC11-3
48. Kjonigsen LJ, Leergaard TB, Witter MP, Bjaalie JG. 2011. Digital atlas of anatomical subdivisions and boundaries of the rat hippocampal region. *Front Neuroinform* 5:2
49. Knapska E, Radwanska K, Werka T, Kaczmarek L. 2007. Functional internal complexity of amygdala: focus on gene activity mapping after behavioral training and drugs of abuse. *Physiol Rev* 87:1113-73
50. Knutson KM, Rakowsky ST, Solomon J, Krueger F, Raymont V, et al. 2013. Injured brain regions associated with anxiety in Vietnam veterans. *Neuropsychologia* 51:686-94
51. Kreutzberg GW. 1996. Microglia: a sensor for pathological events in the CNS. *Trends Neurosci* 19:312-8

52. Kroncke KD, Fehsel K, Kolb-Bachofen V. 1998. Inducible nitric oxide synthase in human diseases. *Clin Exp Immunol* 113:147-56
53. Kumar A, Loane DJ. 2012. Neuroinflammation after traumatic brain injury: opportunities for therapeutic intervention. *Brain Behav Immun* 26:1191-201
54. Li J, Gu L, Feng DF, Ding F, Zhu G, Rong J. 2012. Exploring temporospatial changes in glucose metabolic disorder, learning, and memory dysfunction in a rat model of diffuse axonal injury. *J Neurotrauma* 29:2635-46
55. Lin AP, Liao HJ, Merugumala SK, Prabhu SP, Meehan WP, 3rd, Ross BD. 2012. Metabolic imaging of mild traumatic brain injury. *Brain Imaging Behav* 6:208-23
56. Liu Y, Yao Z, Zhang L, Zhu H, Deng W, Qin C. 2013. Insulin induces neurite outgrowth via SIRT1 in SH-SY5Y cells. *Neuroscience* 238:371-80
57. Liu YR, Cardamone L, Hogan RE, Gregoire MC, Williams JP, et al. 2010. Progressive metabolic and structural cerebral perturbations after traumatic brain injury: an in vivo imaging study in the rat. *J Nucl Med* 51:1788-95
58. Llompart-Pou JA, Raurich JM, Perez-Barcena J, Barcelo A, Ibanez J, Ayestaran JI. 2008. Acute Hypothalamic-pituitary-adrenal response in traumatic brain injury with and without extracerebral trauma. *Neurocrit Care* 9:230-6
59. Loane DJ, Byrnes KR. 2010. Role of microglia in neurotrauma. *Neurotherapeutics* 7:366-77
60. Lochhead JJ, Thorne RG. 2012. Intranasal delivery of biologics to the central nervous system. *Adv Drug Deliv Rev* 64:614-28
61. Maas AIR, Stocchetti N, Bullock R. 2008. Moderate and severe traumatic brain injury in adults. *The Lancet Neurology* 7:728-41
62. Malkesman O, Tucker LB, Ozl J, McCabe JT. 2013. Traumatic brain injury - modeling neuropsychiatric symptoms in rodents. *Front Neurol* 4:157
63. Mantovani A, Sica A, Sozzani S, Allavena P, Vecchi A, Locati M. 2004. The chemokine system in diverse forms of macrophage activation and polarization. *Trends Immunol* 25:677-86
64. Martin EI, Ressler KJ, Binder E, Nemeroff CB. 2009. The neurobiology of anxiety disorders: brain imaging, genetics, and psychoneuroendocrinology. *Psychiatr Clin North Am* 32:549-75
65. Mergenthaler P, Lindauer U, Dienel GA, Meisel A. 2013. Sugar for the brain: the role of glucose in physiological and pathological brain function. *Trends Neurosci* 36:587-97
66. Muhic M, Vardjan N, Chowdhury HH, Zorec R, Kreft M. 2015. Insulin and Insulin-like Growth Factor 1 (IGF-1) Modulate Cytoplasmic Glucose and Glycogen Levels but Not Glucose Transport across the Membrane in Astrocytes. *J Biol Chem* 290:11167-76
67. Nedelcovych MT, Gadiano AJ, Wu Y, Manning AA, Thomas AG, et al. 2018. Pharmacokinetics of Intranasal versus Subcutaneous Insulin in the Mouse. *ACS Chem Neurosci* 9:809-16
68. Needham E, Zandi MS. 2014. Recent advances in the neuroimmunology of cell-surface CNS autoantibody syndromes, Alzheimer's disease, traumatic brain injury and schizophrenia. *J Neurol* 261:2037-42
69. Nimmerjahn A, Kirchhoff F, Helmchen F. 2005. Resting microglial cells are highly dynamic surveillants of brain parenchyma in vivo. *Science* 308:1314-8

70. Ocampo AC, Squire LR, Clark RE. 2017. Hippocampal area CA1 and remote memory in rats. *Learn Mem* 24:563-8
71. Ohsawa K, Imai Y, Sasaki Y, Kohsaka S. 2004. Microglia/macrophage-specific protein Iba1 binds to fimbrin and enhances its actin-bundling activity. *Journal of Neurochemistry* 88:844-56
72. Olesen SP. 1987. Leakiness of rat brain microvessels to fluorescent probes following craniotomy. *Acta Physiol Scand* 130:63-8
73. Osborn AJ, Mathias JL, Fairweather-Schmidt AK, Anstey KJ. 2017. Anxiety and comorbid depression following traumatic brain injury in a community-based sample of young, middle-aged and older adults. *J Affect Disord* 213:214-21
74. Osier ND, Dixon CE. 2016. The Controlled Cortical Impact Model: Applications, Considerations for Researchers, and Future Directions. *Front Neurol* 7:134
75. Pan W, Kastin AJ. 2017. The Blood-Brain Barrier: Regulatory Roles in Wakefulness and Sleep. *Neuroscientist* 23:124-36
76. Parameswaran N, Patial S. 2010. Tumor necrosis factor-alpha signaling in macrophages. *Crit Rev Eukaryot Gene Expr* 20:87-103
77. Plum L, Schubert M, Bruning JC. 2005. The role of insulin receptor signaling in the brain. *Trends Endocrinol Metab* 16:59-65
78. Prevention CfDCa. 2015. Report to Congress on Traumatic Brain Injury in the United States: Epidemiology and Rehabilitation. National Center for Injury Prevention and Control; Division of Unintentional Injury Prevention. , Atlanta, GA.
79. Prut L, Belzung C. 2003. The open field as a paradigm to measure the effects of drugs on anxiety-like behaviors: a review. *Eur J Pharmacol* 463:3-33
80. Recio-Pinto E, Rechler MM, Ishii DN. 1986. Effects of insulin, insulin-like growth factor-II, and nerve growth factor on neurite formation and survival in cultured sympathetic and sensory neurons. *J Neurosci* 6:1211-9
81. Saltiel AR, Pessin JE. 2002. Insulin signaling pathways in time and space. *Trends Cell Biol* 12:65-71
82. Santarsieri M, Kumar RG, Kochanek PM, Berga S, Wagner AK. 2015. Variable neuroendocrine-immune dysfunction in individuals with unfavorable outcome after severe traumatic brain injury. *Brain Behav Immun* 45:15-27
83. Scholten AC, Haagsma JA, Cnossen MC, Olff M, van Beeck EF, Polinder S. 2016. Prevalence of and Risk Factors for Anxiety and Depressive Disorders after Traumatic Brain Injury: A Systematic Review. *J Neurotrauma* 33:1969-94
84. Schulingkamp RJ, Pagano TC, Hung D, Raffa RB. 2000. Insulin receptors and insulin action in the brain: review and clinical implications. *Neurosci Biobehav Rev* 24:855-72
85. Schulingkamp RJ, Pagano, T.C.,Hung, D., Raffa, R.B. 2000. Insuin receptors and insulin action in the brain. *Neuroscience and Biobehavioral Reviews* 24:855–72
86. Shepherd JK, Grewal SS, Fletcher A, Bill DJ, Dourish CT. 1994. Behavioural and pharmacological characterisation of the elevated "zero-maze" as an animal model of anxiety. *Psychopharmacology (Berl)* 116:56-64
87. Siebold L, Obenaus A, Goyal R. 2018. Criteria to define mild, moderate, and severe traumatic brain injury in the mouse controlled cortical impact model. *Exp Neurol* 310:48-57

88. Squire LR. 2009. The legacy of patient H.M. for neuroscience. *Neuron* 61:6-9
89. Swardfager W, Lanctot K, Rothenburg L, Wong A, Cappell J, Herrmann N. 2010. A meta-analysis of cytokines in Alzheimer's disease. *Biol Psychiatry* 68:930-41
90. Tremblay ME, Stevens B, Sierra A, Wake H, Bessis A, Nimmerjahn A. 2011. The role of microglia in the healthy brain. *J Neurosci* 31:16064-9
91. Tucker LB, Burke JF, Fu AH, McCabe JT. 2017. Neuropsychiatric Symptom Modeling in Male and Female C57BL/6J Mice after Experimental Traumatic Brain Injury. *J Neurotrauma* 34:890-905
92. Uemura E, Greenlee HW. 2006. Insulin regulates neuronal glucose uptake by promoting translocation of glucose transporter GLUT3. *Exp Neurol* 198:48-53
93. Unal-Cevik I, Kilinc M, Gursoy-Ozdemir Y, Gurer G, Dalkara T. 2004. Loss of NeuN immunoreactivity after cerebral ischemia does not indicate neuronal cell loss: a cautionary note. *Brain Res* 1015:169-74
94. Unger JW, Livingston JN, Moss AM. 1991. Insulin receptors in the central nervous system: localization, signalling mechanisms and functional aspects. *Prog Neurobiol* 36:343-62
95. Villapol S, Byrnes KR, Symes AJ. 2014. Temporal dynamics of cerebral blood flow, cortical damage, apoptosis, astrocyte-vasculature interaction and astrogliosis in the pericontusional region after traumatic brain injury. *Front Neurol* 5:82
96. von Leden RE, Khayrullina G, Moritz KE, Byrnes KR. 2017. Age exacerbates microglial activation, oxidative stress, inflammatory and NOX2 gene expression, and delays functional recovery in a middle-aged rodent model of spinal cord injury. *J Neuroinflammation* 14:161
97. Walf AA, Frye CA. 2007. The use of the elevated plus maze as an assay of anxiety-related behavior in rodents. *Nat Protoc* 2:322-8
98. Webb NE, Little B, Loupee-Wilson S, Power EM. 2014. Traumatic brain injury and neuro-endocrine disruption: medical and psychosocial rehabilitation. *NeuroRehabilitation* 34:625-36
99. Weeks HR, 3rd, Tadler SC, Smith KW, Iacob E, Saccoman M, et al. 2013. Antidepressant and neurocognitive effects of isoflurane anesthesia versus electroconvulsive therapy in refractory depression. *PLoS One* 8:e69809
100. Werner C, Engelhard K. 2007. Pathophysiology of traumatic brain injury. *Br J Anaesth* 99:4-9
101. Werner H, LeRoith D. 2014. Insulin and insulin-like growth factor receptors in the brain: physiological and pathological aspects. *Eur Neuropsychopharmacol* 24:1947-53
102. Wu XH, Yang SH, Duan DY, Cheng HH, Bao YT, Zhang Y. 2007. Anti-apoptotic effect of insulin in the control of cell death and neurologic deficit after acute spinal cord injury in rats. *J Neurotrauma* 24:1502-12
103. Yoshino A, Hovda DA, Kawamata T, Katayama Y, Becker DP. 1991. Dynamic changes in local cerebral glucose utilization following cerebral concussion in rats: evidence of a hyper- and subsequent hypometabolic state. *Brain Research* 561:106-19
104. Zhang B, Wei YZ, Wang GQ, Li DD, Shi JS, Zhang F. 2018. Targeting MAPK Pathways by Naringenin Modulates Microglia M1/M2 Polarization in Lipopolysaccharide-Stimulated Cultures. *Front Cell Neurosci* 12:531

105. Zhao WQ, Chen H, Quon MJ, Alkon DL. 2004. Insulin and the insulin receptor in experimental models of learning and memory. *Eur J Pharmacol* 490:71-81